Copyright

By

Angela Kelechi Eluwa

2015

The Thesis Committee for Angela Kelechi Eluwa
Certifies that this is the approved version of the following thesis:

Depositional Systems Analysis of the Lower Miocene Interval in Refugio County, Western Gulf of Mexico Basin

APPROVED BY
SUPERVISING COMMITTEE:

David Mohrig, Supervisor

William L. Fisher, Co-Supervisor

Osareni C. Ogiesoba, Co-Supervisor

Depositional Systems Analysis of the Lower Miocene Interval in Refugio County, Western Gulf of Mexico Basin

By

Angela Kelechi Eluwa, B.S.

Thesis

Presented to the Faculty of the Graduate School of

The University of Texas at Austin

in Partial Fulfillment

of the Requirements

for the Degree of

Master of Science in Energy and Earth Resources

The University of Texas at Austin

August 2015

Dedication

To my Dad and siblings.

Acknowledgements

It is with immense appreciation that I thank my supervisors. Despite their very busy schedule, they always took the time to assist me. Dr. David Mohrig gave me tireless support throughout the period of my thesis. His calm way of re-directing me, whenever I got stuck had a great and positive impact on me to keep working. Dr. William Fisher, who was also my academic advisor, provided immeasurable assistance throughout my academic period. I would like to thank Dr. Christopher Ogiesoba for taking me as his *protégé*; he provided the fundamentals and organization of my research.

This thesis was sponsored by the State of Texas Advanced Oil and Gas Resource Recovery (STARR) group of the Bureau of Economic Geology at The University of Texas at Austin. In particular, I would like to express my gratitude to Dr. William Ambrose; he never hesitated to share his expertise whenever I found myself bound by the complexities of this research. Thanks to T.C. Oil Company for the seismic data set and also, thanks to T.C. Oil and IHS companies for the well log data.

I sincerely appreciate the technical assistance provided by Dallas Dunlap, David Smith, and members of the Gulf of Mexico Basin Depositional Synthesis (GBDS) research team – Dr. Jon Snedden and Jonathan Virdell. My smooth sail throughout my graduate program was courtesy my graduate coordinator- Ms. Jessica Smith, thank you very much for your readiness to provide necessary academic information.

To my family, especially my brother Dr. George Eluwa, I won't be here without your love and support. Your belief in me, strengthened my resolve to succeed. To my first mentor, Dr. A.Y.B Anifowose, you laid the academic foundation on which I have achieved this feat. Thank you.

Abstract

Depositional Systems Analysis of the Lower Miocene Interval in Refugio County, Western Gulf of Mexico Basin

Angela Kelechi Eluwa, M.S.E.E.R.

The University of Texas at Austin, 2015

Supervisor: David Mohrig

Co-supervisor: William L. Fisher

Co-supervisor: Osareni C. Ogiesoba

Definition of the environments within a depositional system provides useful information about the possible depositional processes; and in turn helps predict the amount and caliber of sediments transported to the basin. This research analyzes variance attribute maps to identify the different environments of deposition within Refugio County, Texas; this analysis also addresses the possible influence by the San Marcos Arch on Lower Miocene deposition.

The study area is subsurface, Lower Miocene strata of Refugio County situated in the western GOM basin. Numerous variance attribute maps were generated from a three dimensional (3D) seismic volume. These maps reveal that the stratigraphic section is predominantly an expanded regressive phase. The basal Miocene strata that immediately overlie the Anahuac Shale preserve the record of significant shoreline progradation as shown by a thick and laterally extensive complex of amalgamated beach-ridge deposits

associated with longshore transport of sand. These beach deposits are overlain by a thick section dominated by incised valleys fills, and channel and channel-belt deposits. Subtle change in incised valley shape is interpreted to record change in distance or relative proximity to the shoreline.

The logs from 17 wells are integrated with the 3D seismic data to quantify sandstone/shale variability and develop sand maps. The San Marcos Arch is a significant structural feature located towards the northeastern part of the study area. Contoured sand thickness maps of four intervals within the dataset indicate increase in sand thicknesses towards the northeast, indicating that the influence of the San Marcos Arch on sediment deposition had waned by the Lower Miocene.

Table of Contents

List of Figures ix

INTRODUCTION **1**

OBJECTIVES 1

BACKGROUND/PALEOGEOGRAPHY/DEPOSITIONAL HISTORY 4

STRUCTURAL HISTORY 10

METHOD OF INVESTIGATION **13**

CLASTIC DEPOSITIONAL SYSTEMS **18**

DELTAS 18

DELTA CLASSIFICATION 18

Fluvial dominated deltas 18

Wave dominated deltas 21

Tide dominated deltas 21

SHOREZONE 23

STRANDPLAINS 23

INCISED VALLEYS 25

ESTUARY 28

WELL-LOG REFLCTIONS IN DEPOSITIONAL ENVIRONMENTS 30

Deltas 31

Shorezone 31

Incised valleys 31

Estuaries 32

RESULTS **38**

DISCUSSION AND CONCLUSIONS **59**

REFERENCES 62

List of Figures

Figure 1: Regional map of NW Gulf of Mexico showing the different depositional environments. Courtesy Gulf Basin Depositional Synthesis (GDBS) 2013.....3

Figure 2: Deformation and subsidence pattern leading to basin formation. (Galloway, 1989) 5

Figure 3: Sediment supply and dispersal axes for the northwestern and central parts of Gulf of Mexico during the Cenozoic period. Red dashed rectangle shows the approximate position of the study area. CZ = Carrizo; RG = Rio Grande. (Modified from Galloway et al. 2000) 6

Figure 4: Progressive Cenozoic shelf edge positions and sand-rich depocenters of northwestern Gulf of Mexico. (Winker 1982 in Galloway 1989) 7

Figure 5: Paleogeography and principal depositional systems of the study area. (Galloway et al., 2000).....8

Figure 6: Generalized dip-oriented stratigraphic cross section through the Rio Grande depocenter, northwestern Gulf Coast sedimentary wedge. (Galloway, 1989). 9

Figure 7: Map showing some principal structural features in Cenozoic GOM. (Halbouty, 1966) 11

Figure 8: Area map of San Marcos map showing position of Refugio County (in red rectangle). Approximate distance was calculated using the map. (Halbouty, 1966) 12

Figure 9: Base map of Refugio County. See figure 1 for location map. Yellow circles represent the positions of 17 Well logs in the study interval. The well locations are represented this way in all maps. 14

Figure 10: An arbitrary seismic line showing horizons mapped and some well logs with Spontaneous Potential (red), Gamma (black), Resistivity (blue) 15

Figure 11. Miocene stratigraphy chart for the GOM basin. Complete chart shows the entire stratigraphic sequences for the Cenozoic Period. Courtesy Gulf Basin Depositional Synthesis (GBDS) 2013. 16

Figure 12: The distribution of major coastal depositional environments. Prograding (regressive) environments and retrograding (transgressive) environments are highlighted. (Boyd et al., 1992) 19

Figure 13: Delta sub-environments: a) details of clinoforms formed in each sub-environment, average distance covered by each section and extent of dominant coastal processes. b) Map view of the typical components of a delta (Goodbred and Saito 2012). 20

Figure 14: An example showing the morphology of a fluvial dominated delta system. (Fisher et al 1969) 21

Figure 15: Wave- influenced delta process formation. (Bhattacharya and Giosan 2003) 22

Figure 16: Typical shorezone and wave dominated delta vertical succession. A) shorezone facies succession. B) Wave dominated delta facies succession. (Modified from Clifton 2006, Bhattacharya and Walker 1991) 24

Figure 17: Typical shorezone profile. Red circles mark the principal environments and their facies. (Walker and Plint, 1992) 24

Figure 18: Illustrative models showing the typical strandplain environments of deposition. (Galloway and Cheng, 1985 in Ambrose. and Tyler, 1985) 25
Figure 19: Longitudinal profile of facies distribution in an incised valley. (Congxian et al., 2006) 26
Figure 20: Facies sucession types within incised valley systems. (Congxian et al., 2006) 27
Figure 21: Schematic illustration of (A) simple and (B) compound incised-valley systems. Numbers 1-3 refer to successive episodes of cutting and filling within the incised valley. PS= parasequence; FS = flooding surface. (Zaitlin et al. 1994) 28
Figure 22: An illustration of a typical estuary environment. A) An estuary is influenced by both marine and fluvial environments. B) The resultant depositional environment with fluvial derived channels and marine influenced sand bars. C) Estuaries contain heterogeneous deposits from two sources. (Dalrymple et al. 1992 in Olariu 2014).....29
Figure 23: An example of gamma ray and spontaneous potential logs. Note the difference in response between both logs in the sand-shale intervals and also in the hydrocarbon saturated zone. (Fongngern 2011).....32
Figure 24: Typical well log response in fluvial and wave delta environments. Deposits are overlain by MFS. (Bhattacharya and Walker 1991 in Olariu 2014) 33
Figure 25: Highstand delta well log pattern. (Bhattacharya and Walker 1991) 34
Figure 26: Well log through a shoreface environment. (Modified from Bhattacharya and Walker 1991).....35

Figure 27: Typical dip section of incised valley fill and well log pattern. (Modified from Allen and Posamentier, 1993 in Olariu 2014 and Fongngern 2011). 36
Figure 28: Well log pattern in an estuarine depositional environment. (Bhattacharya 1993) 37
Figure 29: seismic attribute comparison maps for H7, a) is a spectral decomposed map generated using the variance volume .b) is spectral decomposed map generated using the seismic volume. For corresponding variance attribute map, see figure 38a. The channels are more visible in a. Both maps are at a frequency of 25 Hz.....39
Figure 30: seismic attribute comparison maps for H7, b) is a spectral decomposed map at a frequency of 25Hz generated using the seismic volume. c) RMS amplitude map. The channels are more visible in a. Note that the channels are more visible in a, than in b, and features in b are more visible than in c. For corresponding variance attribute map, see figure 38a.....40
Figure 31: Amplitude-variance map for H2; Anahuac shale interval. See figure 10 for horizons positions 41
Figure 32: Coarsening upward to blocky well log pattern observed between H2 and H3. Purple arrows highlight the well log patterns. 42
Figure 33: Amplitude-variance map of H5. Shoreline oriented deposits. Purple line indicates thickness trend shown on the isochron map. 43
Figure 34: Isochron map between H3 and H5. Warm colors are low values, cool colors are higher values. 44
Figure 35: Net-sand isopach map between H3 and H5.....45

Figure 36: Variance attribute map for H4 showing first occurrence of fluvial deltaic environment.. 47
Figure 37: Variance attribute map for H5. Presence of numerous channels indicate further in-land position of the shoreline.....48
Figure 38a: a) Amplitude variance map of H7 showing sinuous channels characterized by minimal lateral migration, marked up areas in red are shown in figure 38b 49
Figure 38b: b) Northeast-Southwest inclined feature of the short-lived strandplain. c) distinctive channel present in the map northern axis for H7 50
Figure 38c: Figure c shows some features are more visible in the spectral decomposed variance attribute maps. d) Figure d highlights the channel featured in c. 51
Figure 39a: Variance attribute map for H8 showing sinuous channels and valley cuts. The red marked out portion is shown in figure 39b.....52
Figure 39b: Sinuous channels featured in H8 extending to the basin.....53
Figure 40a: Variance attribute map for H9 featuring large channels. The red marked out portion is shown in figure 40b. 54
Figure 40b: Numerous channels present within the H7 interval.....55
55
Figure 41a: Variance map for H11; larger valley scours appear in Younger intervals. Red dashed rectangle highlights some incisional features. See figure 41b.....56
Figure 41b: Large west-east trending incisional features in H11 57
Figure 42: Variance map for H15 showing channels and valley cuts.....58

INTRODUCTION

OBJECTIVES

The Gulf of Mexico (GOM) basin has been intensively studied; however, unexplained complexities remain. The objective of this project is a detailed depositional analysis of the Miocene interval within Refugio County area to contribute to the resolution of one of these GOM geological complexities. Refugio County is located along the coastline of the Gulf of Mexico in the northeastern part of the Rio Grande basin (Figure 1).

This research defines the depositional framework of the Miocene in Refugio County with emphasis on identifying regressive and transgressive cycles to recognize depositional episodes. Recognition of the depositional environment is based on morphologic and evolutionary components, as classified by Boyd et al (1992). This classification is founded on dominant coastal processes; it predicts responses in geomorphology, facies and stratigraphy; identification of these responses help to group them into regressive and transgressive categories - {sediment transport in response to sea level changes, sediment influx and accommodation space}. With the use of a three dimensional seismic data and well logs, I examined depositional patterns though time, the structural and stratigraphic features present, the emergence, orientation and size of channels and channel belts.

In addition, I examined the influence of the San Marcos Arch on deposition. The Arch is a basement structural feature located towards the northeastern part of the study area. Halbouty (1966) was of the opinion that the absence of salt controlled sediment accumulations and thinning of sediment thickness towards the Arch prevails in the Wilcox group, Frio and Miocene deposits; therefore the stratigraphic and structural

influence of the arch extends to the present GOM basin. The seismically imaged stratigraphy of the Miocene Refugio County shows no influence associated with the Arch. So, there may still be a structural signal that is best shown by thickness change in the coastal deposits, but the Arch itself is not an influence in any of the geometries associated with the depositional units.

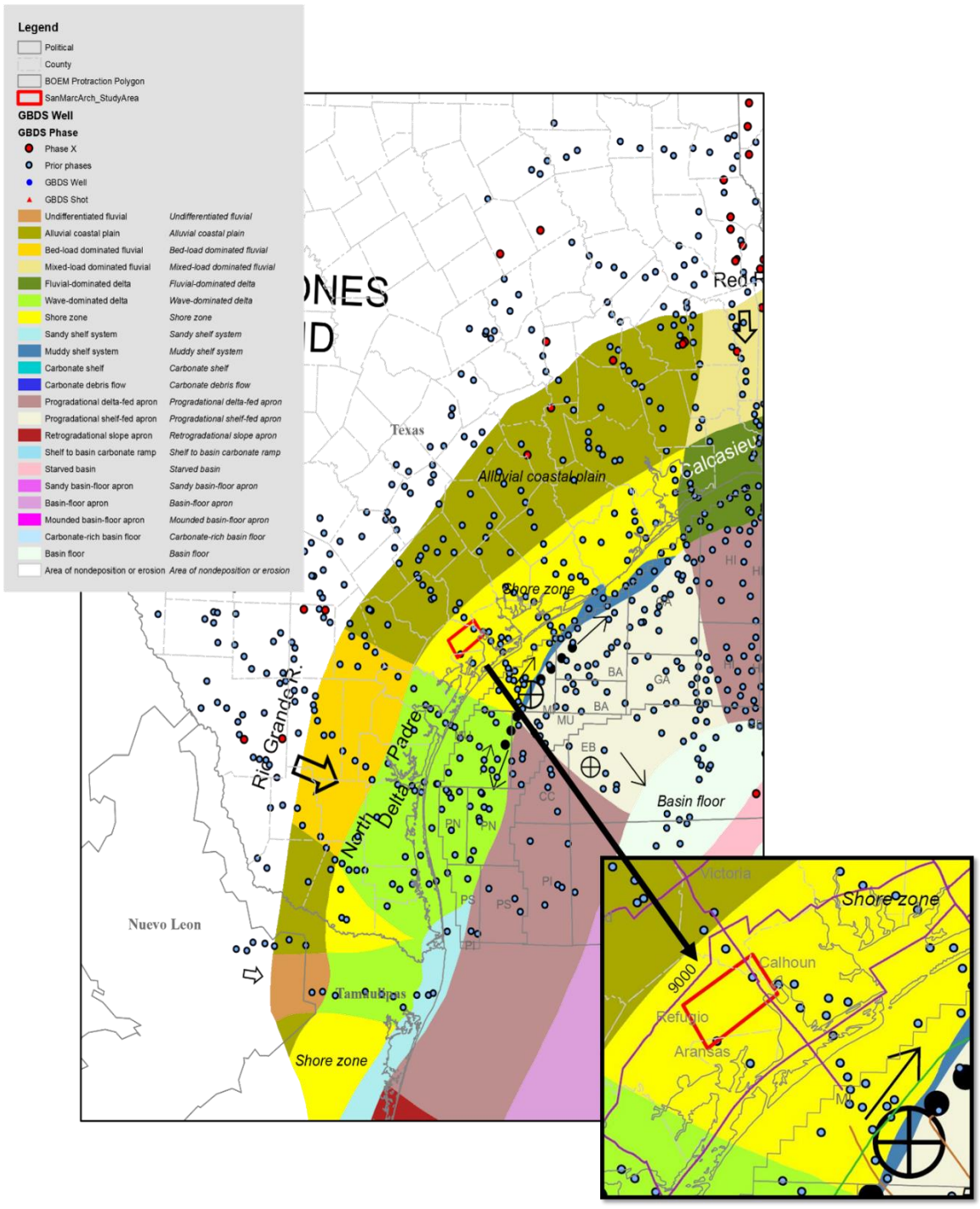

Figure 1: Regional map of NW Gulf of Mexico showing the different depositional environments. Courtesy Gulf Basin Depositional Synthesis (GDBS) 2013

BACKGROUND/PALEOGEOGRAPHY/DEPOSITIONAL HISTORY

Galloway (1987, 1989) suggested that the GOM basin was created by rifting, followed by thermal subsidence of underlying transitional crust to oceanic crust. More accommodation space was created by flexural loading from sediment deposition, allowing for progradation of inner shelf facies and further seaward extension of the shelf margin (Figure 2).

Miocene deposition in the GOM basin is characterized by basin stability; sediment influx, dispersal rate, and shelfal out-building were modulated by eustatic cycles. Sediment provenance (Figure 3) of the northwestern part of the GOM basin during the Paleocene has been attributed to regional uplift and tectonism within the continental interior of western North America (Galloway, 1989). During this time, the geographic dispersion of depocenters around the northwest and central Gulf margins reached their greatest extent. The Rio-Grande, Houston, and Mississippi embayment are the major depocenters in the northwestern GOM basin. (Figure 4)

The North Padre and Norma deltas (Figure 5) were the prominent wave-dominated shore-zone systems in the Rio Grande axis; narrow shelves surrounded these deltas, which contained high volumes of sediment (Galloway et al., 2000). As these deltas prograded, they created sand-rich wedges separated by updip tongues of marine shale that were deposited during transgression and flooding of the shelf. These successions of sandy wedges and marine shale reflect the idealized repetitive nature of Cenozoic deposition (Figure 6). Successive episodes of progradation further builds the shelf edge basinward and successive transgression does not reach as landward as its antecedent (Galloway, 1989).

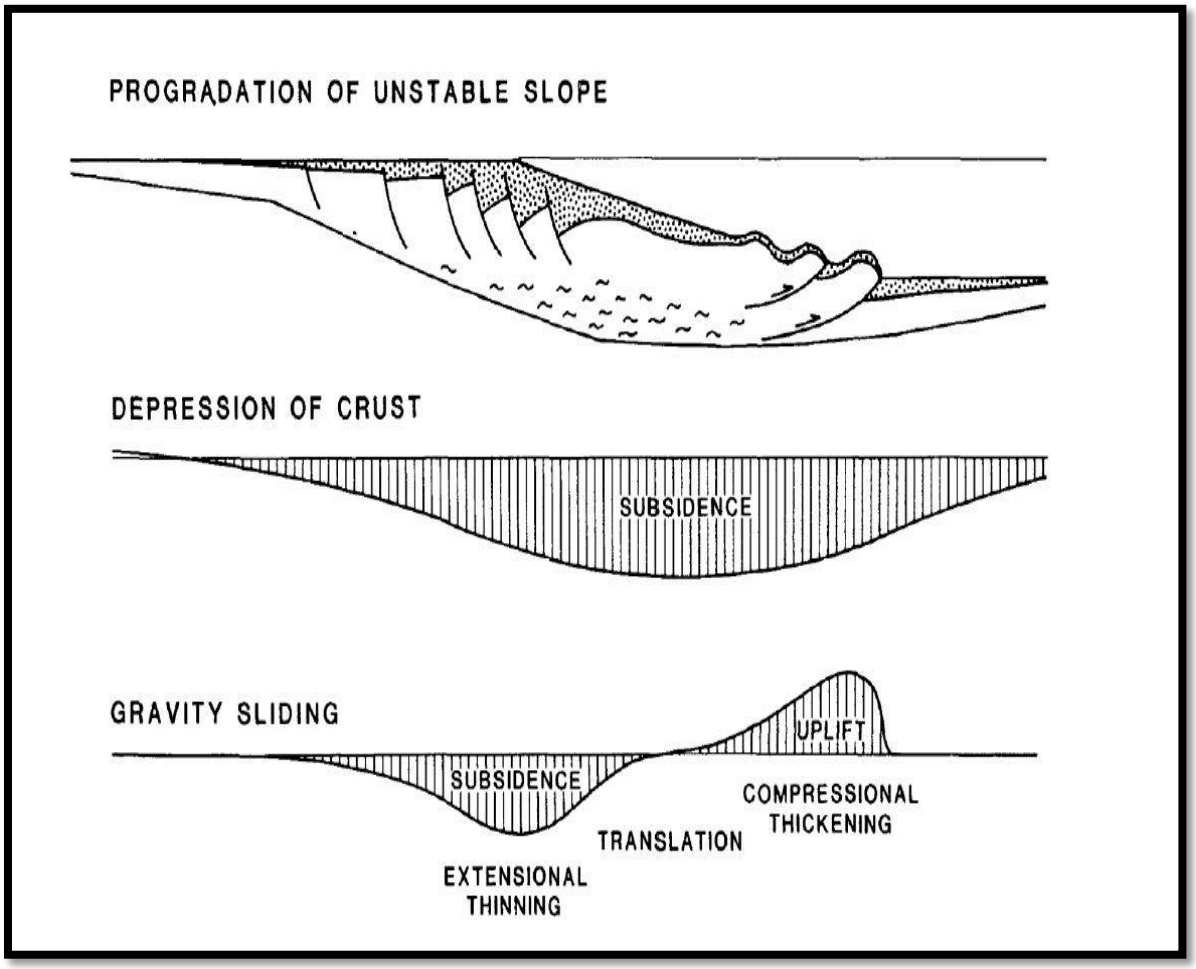

Figure 2: Deformation and subsidence pattern leading to basin formation. (Galloway, 1989)

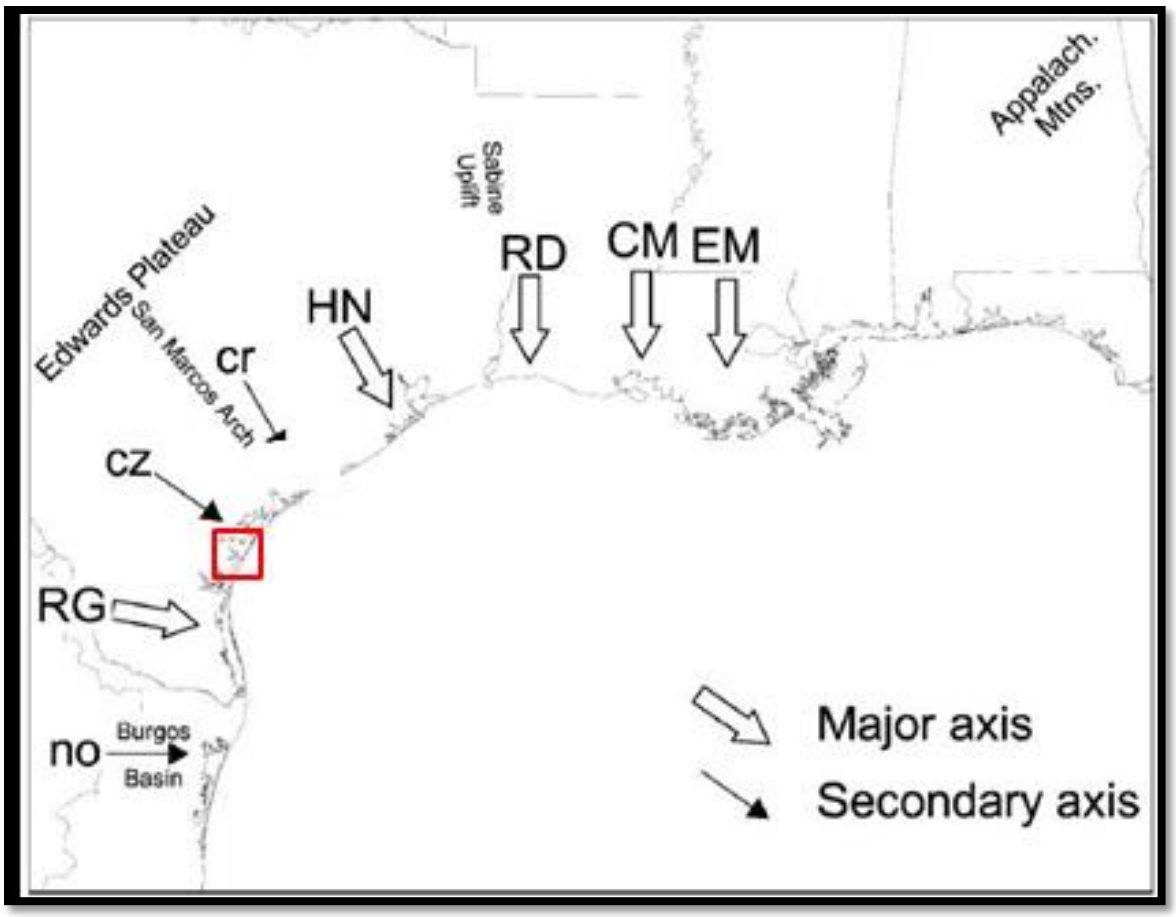

Figure 3: Sediment supply and dispersal axes for the northwestern and central parts of Gulf of Mexico during the Cenozoic period. Red dashed rectangle shows the approximate position of the study area. CZ = Carrizo; RG = Rio Grande. (Modified from Galloway et al. 2000)

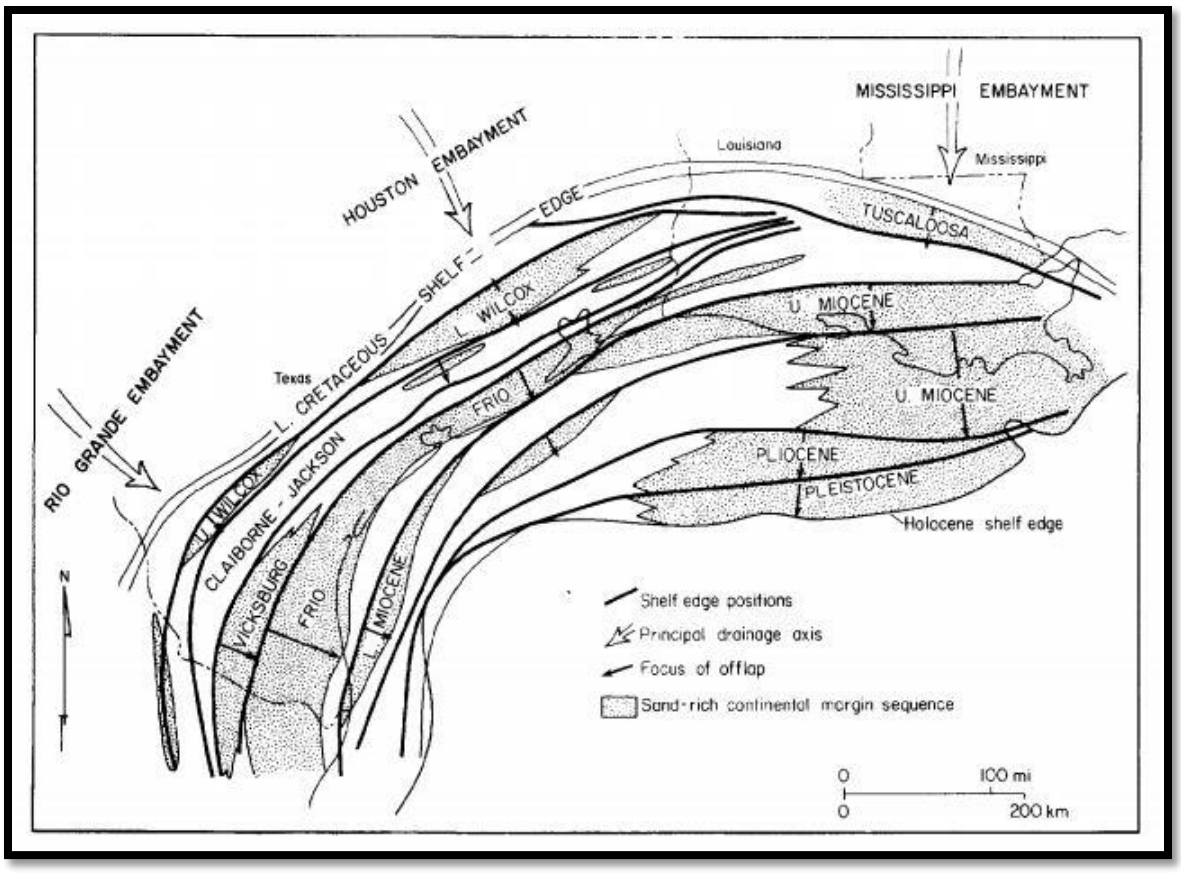

Figure 4: Progressive Cenozoic shelf edge positions and sand-rich depocenters of northwestern Gulf of Mexico. (Winker 1982 in Galloway 1989)

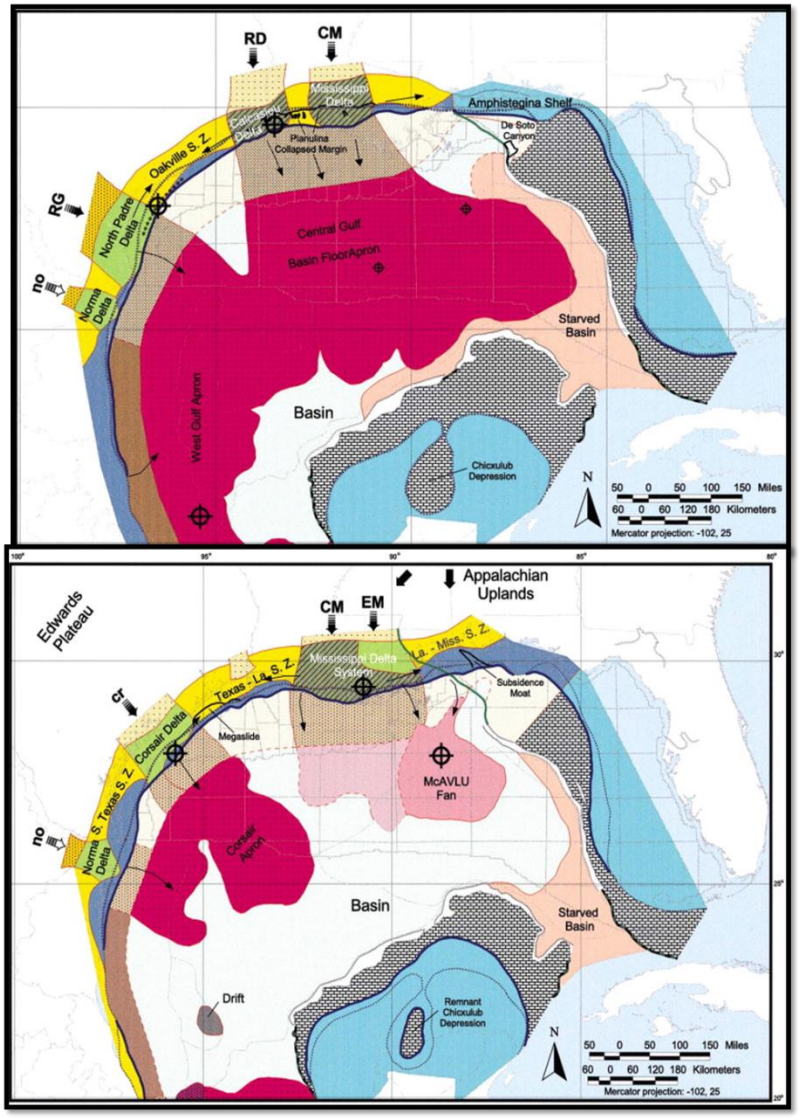

Figure 5: Paleogeography and principal depositional systems of the study area. (Galloway et al., 2000)

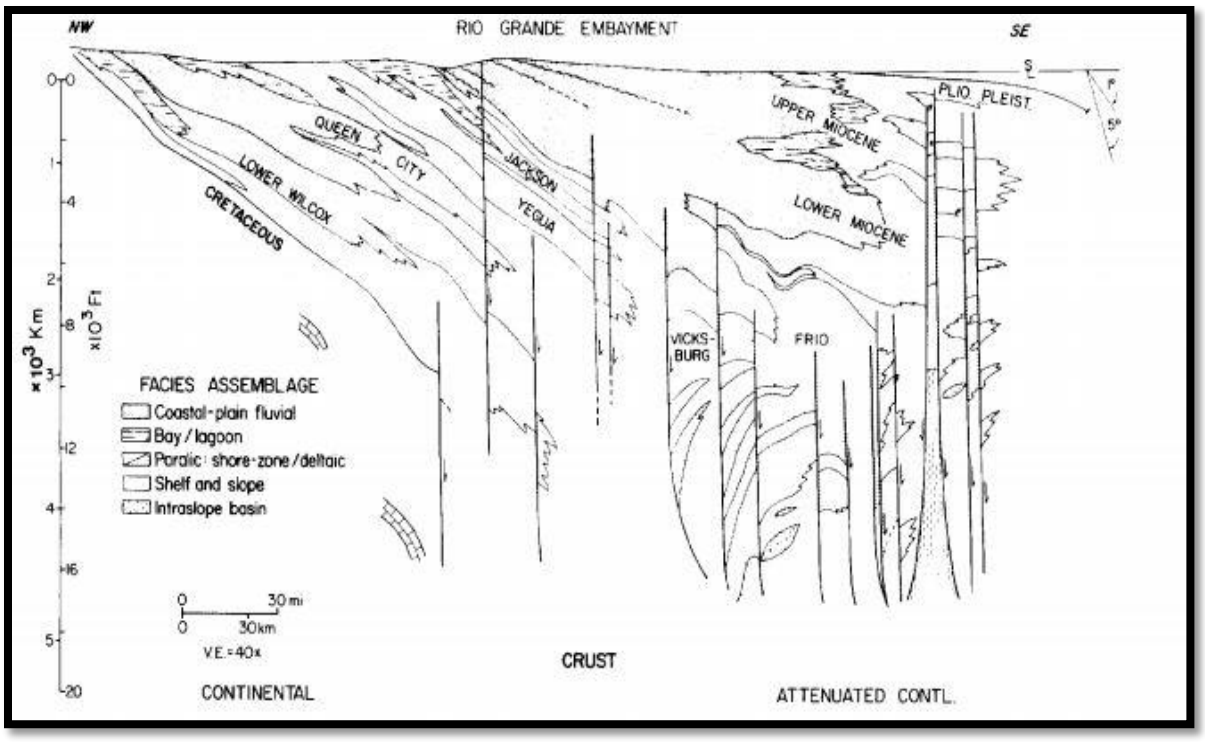

Figure 6: Generalized dip-oriented stratigraphic cross section through the Rio Grande depocenter, northwestern Gulf Coast sedimentary wedge. (Galloway, 1989).

After the Anahuac Shale transgression, the Lower Miocene depositional succession includes fluvial systems, which served as direct supply of sediments to the GOM basin. These systems contain reworked Cretaceous and older Cenozoic debris sourced from uplift of the Edwards Plateau and adjacent inner coastal plain. This depisode also contains barrier and strandplain systems; longshore currents reworked and redistributed sand (both bed load and suspended sediments) along the shelf edge and slope. These currents served as sediment transport media within the basin, albeit at a slower rate than the fluvial systems. A short-lived transgressive episode at about 18 Ma divides the Lower Miocene into two sequences, Lower Miocene 1 and 2 (LM1 and LM2).

During the Middle Miocene, high rate of deposition was recorded. The eastern region was favored as sediment supply from western GOM to the northwest was pruned by the Rio Grande Rift. The parched northern axis of the Rift was responsible for the low volume of sediments transported from the highland to this axis. Nevertheless, sediments from the revived Appalachian Mountains sourced deposition towards the northwestern axis of the Gulf basin which compensated for its initial sediment deficiency at the beginning of the Middle Miocene (Galloway et al. 2011). Sediment input was centered in the Burgos basin in the northwestern GOM basin. The prominent delta system further prograded the shelf margin about 25 mi (40 km). The wave- dominated Corsair delta, advanced about 30 mi (50 km) depositing its thickest sands along the fault zone. This sequence was also capped by a regional transgression of the shelf margin.

The Upper Miocene records more sediment accumulation in the central Mississippi and east Mississippi portion of the GOM basin. Despite the sediment dispersal shift from the northwestern part of the GOM basin, its margin was dominated by a broad sandy strandplain. This was derived from reworked sediments from the shrunken Coarsair, Rio Grande and Norma deltas and also from the Mississippi system.

STRUCTURAL HISTORY

The Cenozoic period of the northern GOM basin houses most of the complex structural features (Galloway 2008). Strike–aligned growth-fault systems beneath the coastal plain, clustered shallow salt stocks canopies beneath the slope region are some of the structural features that are present within the GOM basin. These structures make good stratigraphic and structural trap systems for hydrocarbons, creation of minibasins and also, influence deposit thickness variability.

The San Marcos Arch is an extension of the Llano Uplift; it separates the Houston and Rio Grande basins (Figure 7); and is on the northeastern axis to the Refugio County (Figure 8). Sediment accumulation thins with proximity to and over the arch, this effect is significant from the Jurassic to the Miocene periods (Halbouty, 1966). The Arch is house to several oil and gas exploration and exploitation activities owing to its wealth of stratigraphic and structural traps.

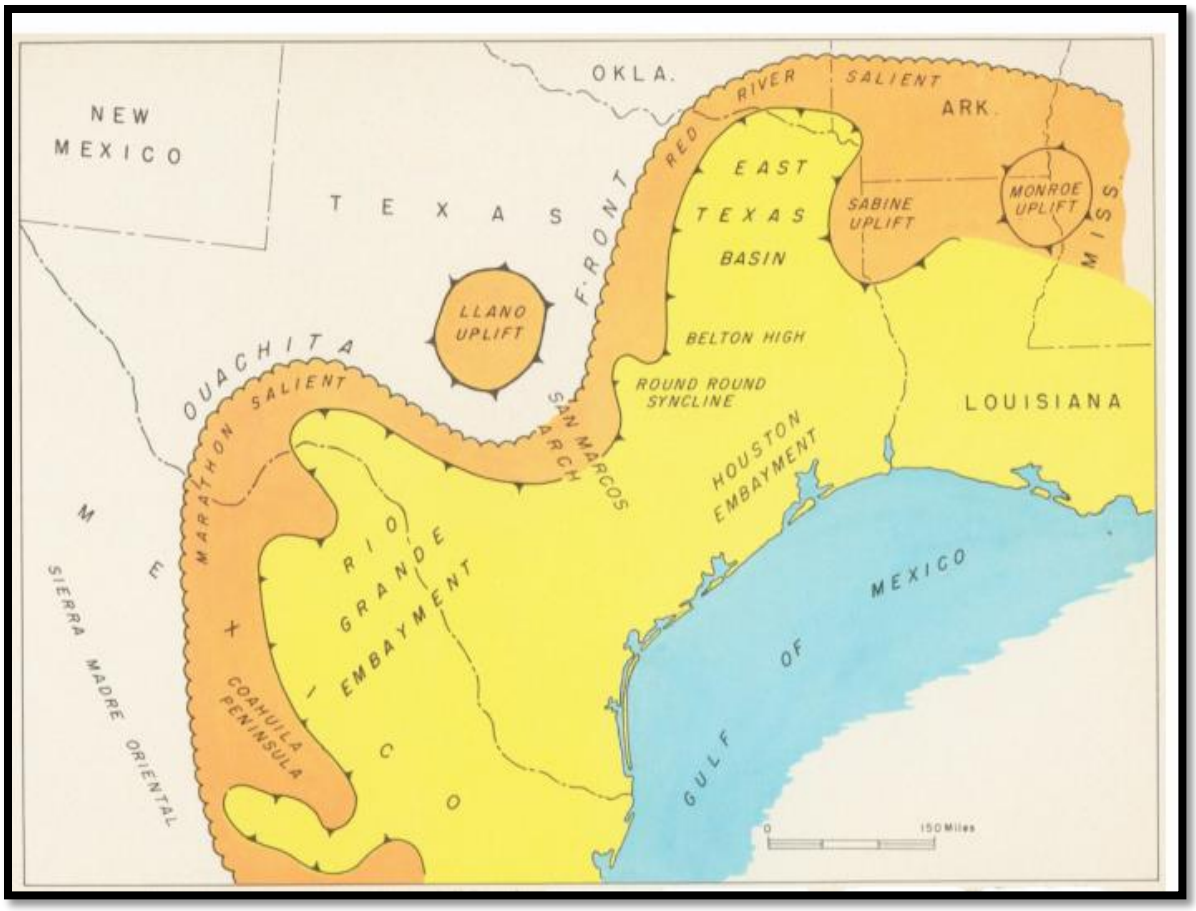

Figure 7: Map showing some principal structural features in Cenozoic GOM. (Halbouty, 1966)

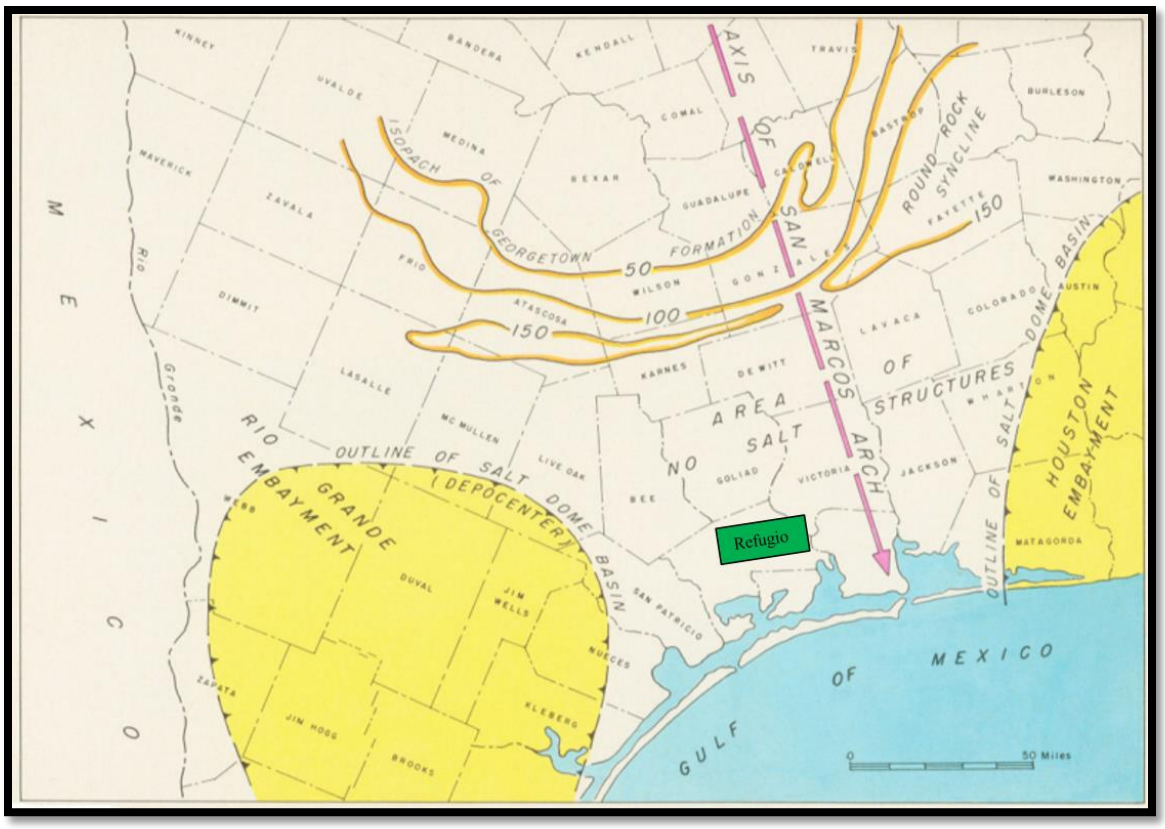

Figure 8: Area map of San Marcos map showing position of Refugio County (in red rectangle). Approximate distance was calculated using the map. (Halbouty, 1966)

METHOD OF INVESTIGATION

The data set used is a three-dimensional (3D) seismic volume of about 106 square miles (275 square kilometers), with bin size 25 m by 25 m, dominant frequency range of 30 to 45 Hz, and typical vertical resolution of about 53 to 70 ft. (16 to 21 m). I used the Landmark software to define and analyze structural and stratigraphic architecture within the dataset. Data quality was adequate. The area of interest covered a depth of 1050 ft. to about 5000 ft. (about 400 to 1500 milliseconds): the top of the Anahuac Shale to the top of the Miocene interval. 17 wireline logs were integrated within the seismic data (Figure 9); 15 of them had a length exceeding the depth of interest (Figure 10). I used gamma ray, spontaneous potential, and resistivity curves as guides in mapping some horizons (Figure 10); notably the base and top of the Anahuac Shale. Well control data from this area was provided by the Gulf Basin Depositional Synthesis (GBDS) research group; this age data indicates that the entire studied section positioned above the Anahuac Shale is Early Miocene. Regional correlations confirm that all deposits studied above Anahuac are bounded above by the Middle Miocene horizon, making the entire section Early Miocene in age. The well log correlation to the Anahuac Shale was aided by the stratigraphic section benchmark chart also courtesy the (GBDS) research group (Figure 11). The remaining 15 horizons were picked at strong amplitude events separated vertically by 30-100 milliseconds. All of the picked horizons were interpolated and filtered.

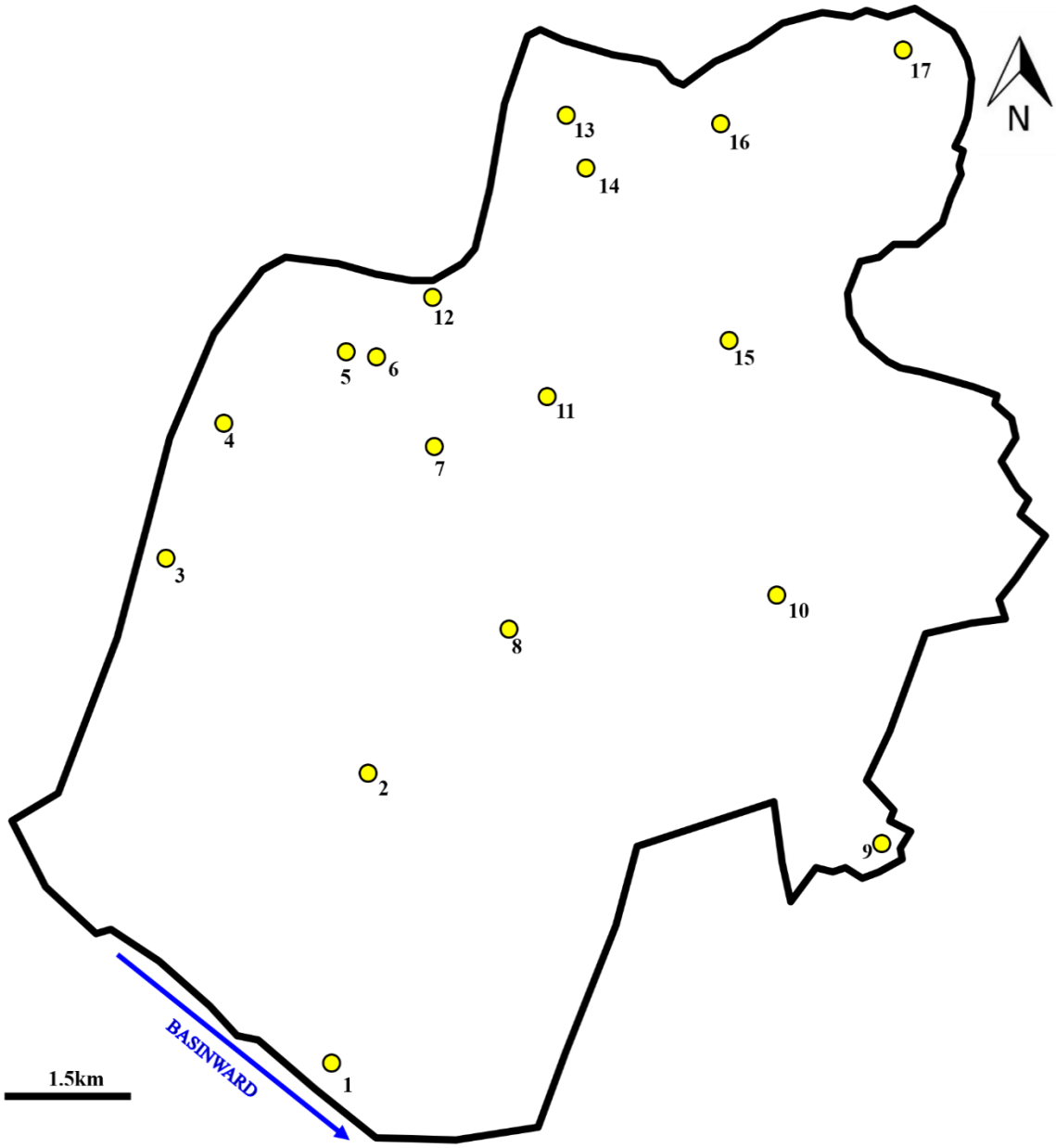

Figure 9: Base map of Refugio County. See figure 1 for location map. Yellow circles represent the positions of 17 Well logs in the study interval. The well locations are represented this way in all maps.

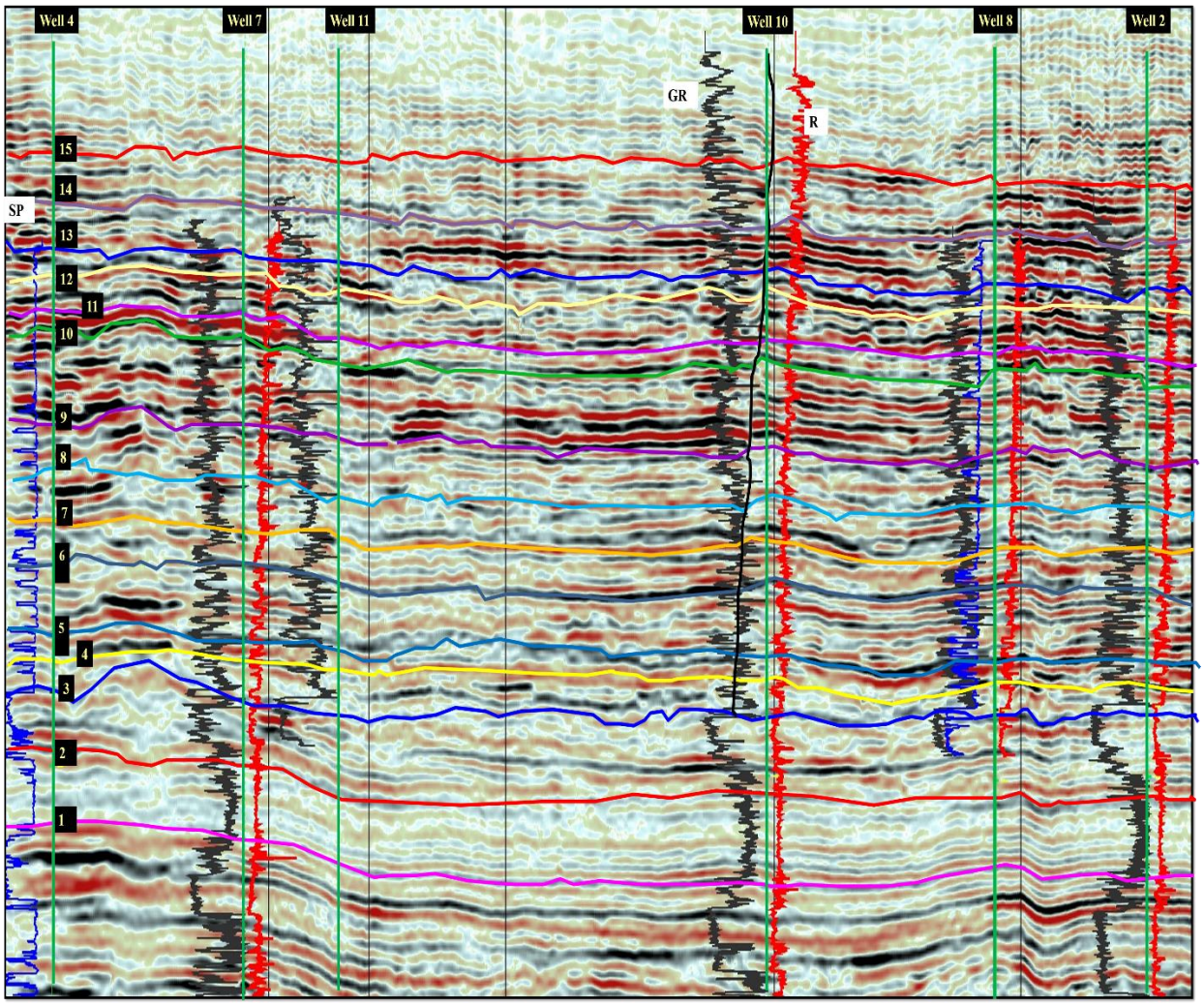

Figure 10: An arbitrary seismic line showing horizons mapped and some well logs with Spontaneous Potential (red), Gamma (black), Resistivity (blue)

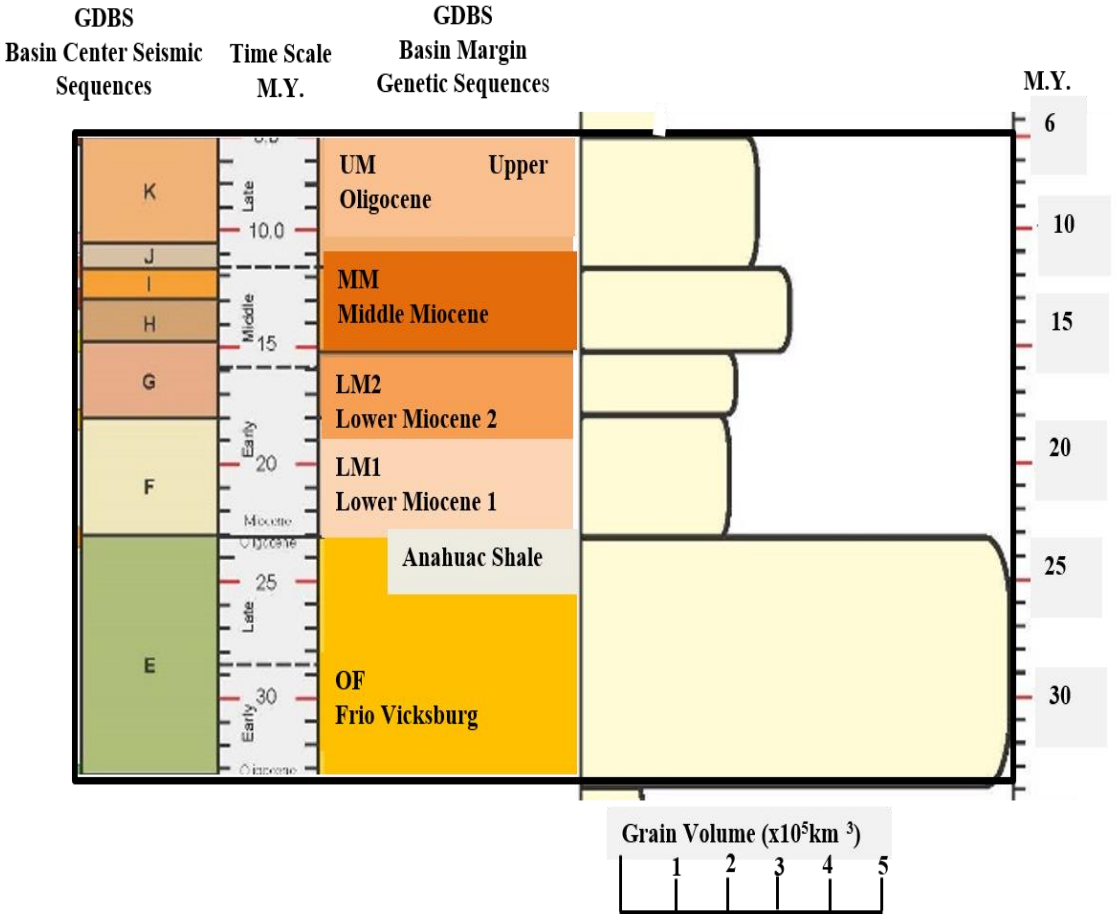

Figure 11. Miocene stratigraphy chart for the GOM basin. Complete chart shows the entire stratigraphic sequences for the Cenozoic Period. Courtesy Gulf Basin Depositional Synthesis (GBDS) 2013.

The mapped horizons were converted to various seismic attributes to identify the one that would yield the best visualization of relevant features within the data. Some of the attributes experimented with in this study include variance, root mean squared amplitude (RMS), and spectral decomposition. The variance attribute is similar to the semblance but gives better resolution than semblance. It is used to detect lateral seismic changes that often relate to geologic changes such as faults, facies changes and other geologic patterns. The attribute volume was generated in Petrel and loaded into the

Seiswork application in Landmark. RMS extraction detects major stratigraphic and lithologic changes, typically sand/shale ratio. Seismic attribute extraction maps were created between horizons and and along horizons using a 16 millisecond window.

The spectral decomposition tool generates several volumes from a single volume input and each of these volumes represents a different frequency band (D. Subrahmanyam and P.H. Rao, 2008). Smaller structures are more visible at higher frequencies and larger structures are visible at lower frequencies. The seismic volume and variance attribute volume were individually used as input volumes. Spectra1 decomposed maps and spectra1 decomposed variance maps were generated along each horizon using a 16 millisecond window, for a frequency range of 0 – 125 Hz.

In order to determine the effect of the San Marcos Arch to sedimentation, I made use of the gamma ray logs to make quantitative sand estimates. The method entails the following steps: (1) Determine gamma ray sand cut-off value in each well. (2) Using the cut-off value, sand-rich interval thicknesses are added together to give net sand thickness within the interval of interest. The interval of interest referred to in this case is an interval bounded by two horizons. Eight horizons were used as reference intervals, and sand intervals defined by the cut-off gamma ray value, were counted in each well between two horizons. Total sand thickness for each interval was individually annotated against its reference well; this was used to produce contoured net sand maps.

CLASTIC DEPOSITIONAL SYSTEMS

The shelf region of the continental margin consists of different depositional environments; and are classified as coastal and shallow marine (Figure 12); few of them, with relevance to this study will be discussed. The creation of these environments is based on certain factors; such as sea level changes, regression and transgression, sediment caliber and influx, evolutionary and morphological changes based on dominant coastal processes (Boyd et al., 1992).

DELTAS

The deltaic environment represents sediments discharged by a river into a standing body of water. With more sediment influx, progradation occurs across the shelf, some of these deposits form subaerially and some are formed subaqueously. There are four geomorphic environments of deposition; predelta, delta plain, delta front and prodelta (Figure 13); the prodelta is the most proximal to the receiving basin (Bhattacharya, 2006). Deltas are subdivided into three; fluvial, wave and tide dominated deltas. This classification represents the dominant marine processes that occur at the river mouth bar.

DELTA CLASSIFICATION

Fluvial dominated deltas

Fluvial dominated deltas are not morphologically influenced by waves and tides. Therefore multiple coeval distributary channels form, some with wide orientation. Channel pattern is sinuous to anastomose. A lobate or elongate shaped delta is usually

formed (Figure 14) and this concentrates sediments into a smaller surface area; sediments deposition into the basin is faster when compared to a wave dominated delta.

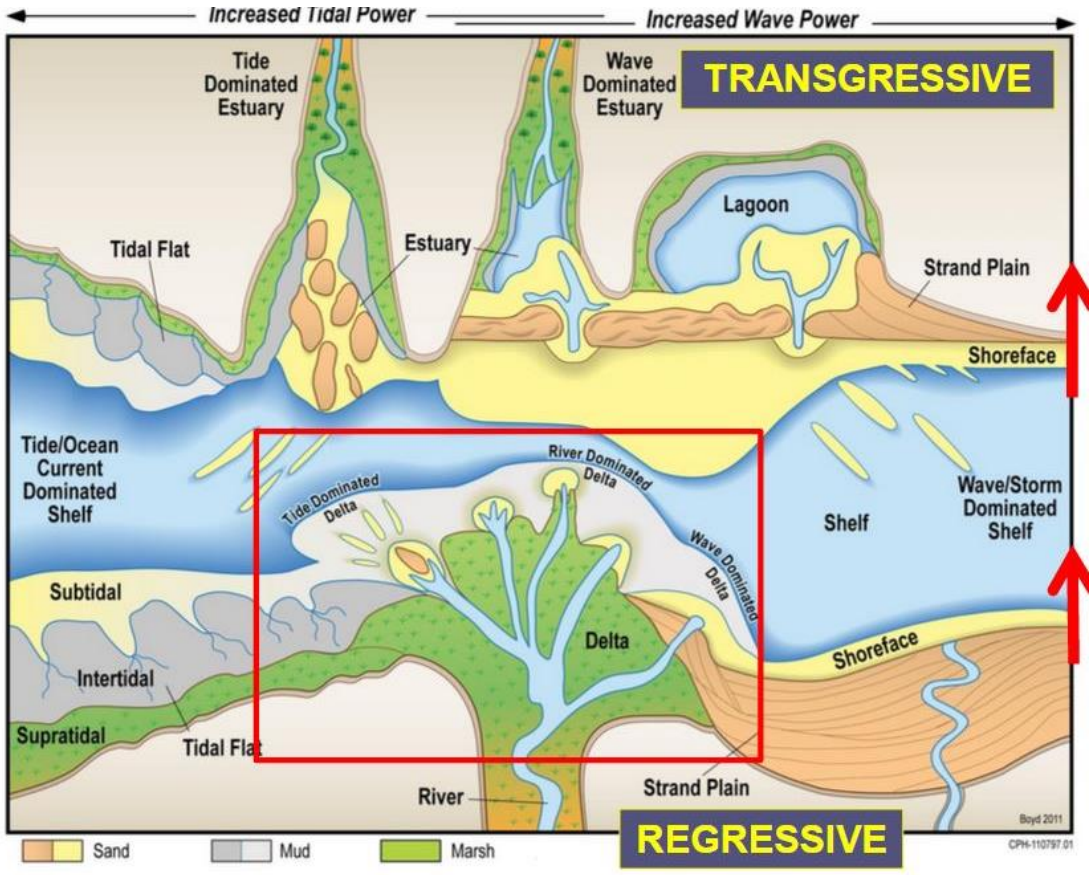

Figure 12: The distribution of major coastal depositional environments. Prograding (regressive) environments and retrograding (transgressive) environments are highlighted. (Boyd et al., 1992)

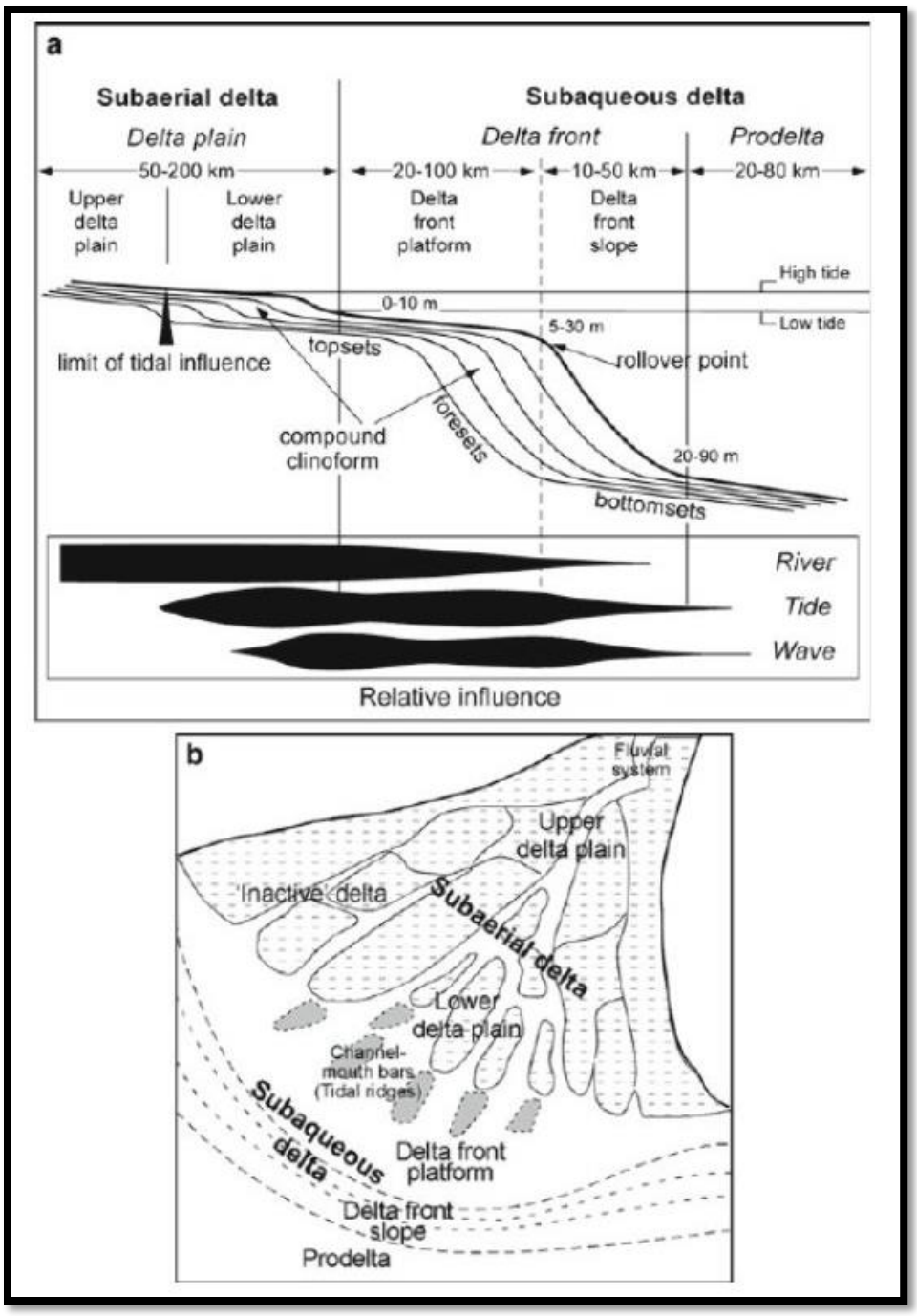

Figure 13: Delta sub-environments: a) details of clinoforms formed in each sub-environment, average distance covered by each section and extent of dominant coastal processes. b) Map view of the typical components of a delta (Goodbred and Saito 2012).

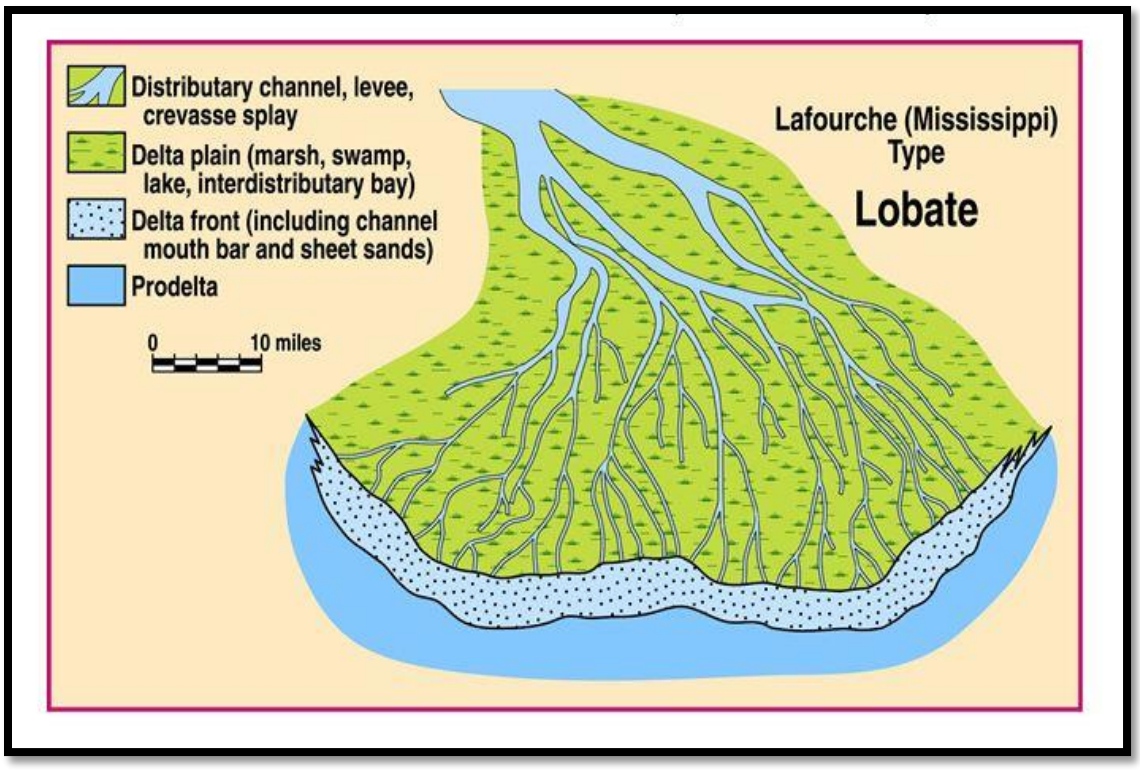

Figure 14: An example showing the morphology of a fluvial dominated delta system. (Fisher et al 1969)

Wave dominated deltas

Waves deflect sediment from the river mouth, with the influence of longshore wave energy. Deposition occurs on both sides of the distributary channels generally referred to as sand spits (Bhattacharya and Giosan, 2003). This generally results in massive sand accumulation in a shoreline parallel position (Figure 15), and this leads to the development of sandy beaches by longshore bars.

Tide dominated deltas

The tide dominated delta environment contains tidally reworked deposits. Channels have few distributary channels that are usually short lived. This environment forms during a highstand period of the sea level and thus usually subaqueous. The

heterolithic nature of sedimentary successions generally present in tide dominated deltaic settings, is formed as a result of the typical inconsistency of tidal energy level (Goodbred and Saito 2012). In tide dominated deltas, mud deposits are predominant in the prodelta and also occur as overbank deposits (Bhattacharya, 2006).

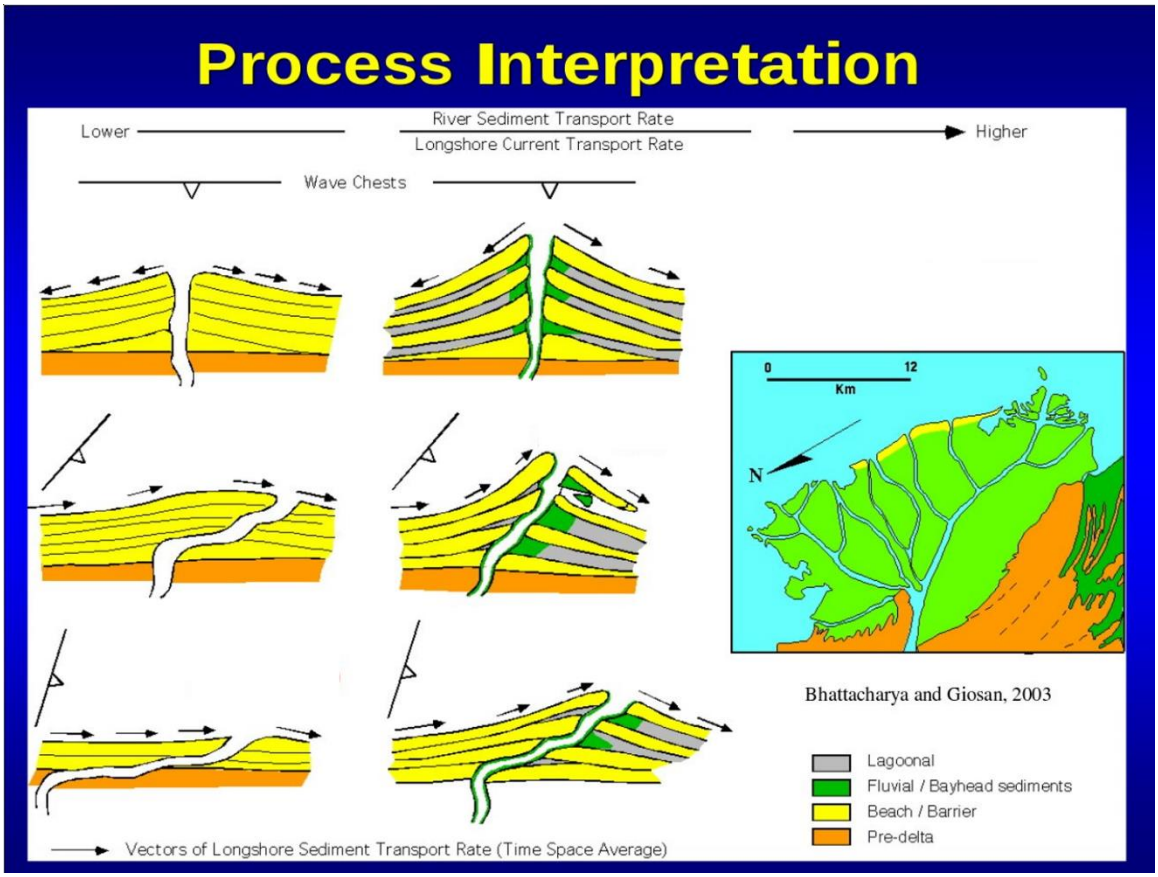

Figure 15: Wave- influenced delta process formation. (Bhattacharya and Giosan 2003)

SHOREZONE

The shorezone depositional section is created by wave processes and has similar lithological facies to a wave dominated delta (Figure 16). Slower rate of sediment influx may inhibit progradation rate; sediment reworking by waves thrives in this condition and this leads to extensive shorezone formation. The foreshore, shoreface and off-shore (Figure 17), are the three wave energy defining limits that make up the shorezone environment (Walker and Plint, 1992). In terms of grain size and facies, the shoreface is a transitional marker between the two end-member environments; typically, a change from sand to mud on the seaward extent of the shorezone.

STRANDPLAINS

Strandplains represent the regressive marine reworked depositional features usually located in a coastal plain environment. They are generally created by redistribution of river mouth sediments by longshore currents. Strandplains are classified based on the degree of sediment heterogeneity and facies architecture (Figure 18); they are grouped into beach-ridge plains and Chenier plains (Ambrose and Tyler, 1985).

The beach-ridge complex is a strike- elongate mass of prograded beach ridges, containing three sub-complexes; a sandy beach-ridge complex, a sandy shoreface and a transecting fluvial-deltaic complex. The beach-ridges contain massive and mostly homogenous thick beach and dune sands. Fluviodeltaic channels cutting through the beach consists of upward-fining channel sandstones.

Chenier plains consist are part of the sandy strandplain system. They are generated from wave reworked sand deposits and are characterized by mud flat intrusions (Owen D.E. 2008). Well log signature is usually characterized by an upward-fining trend. Other sub-complexes include; Chenier strike elongated sand bodies and fluvioestuarine complexes.

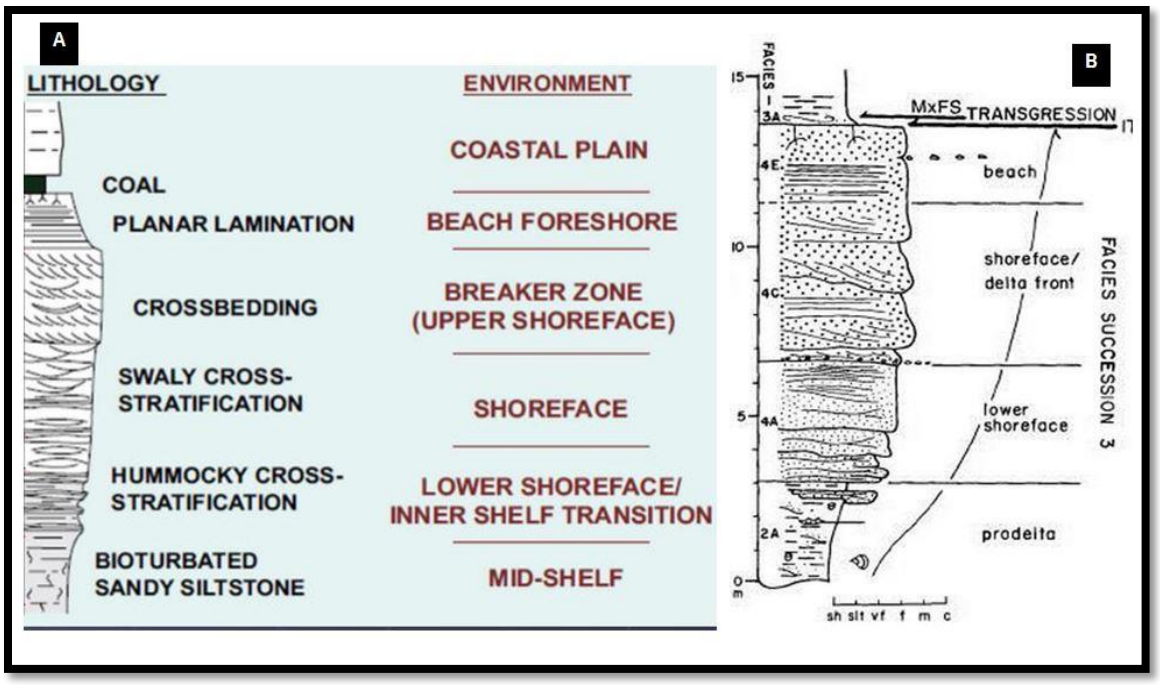

Figure 16: Typical shorezone and wave dominated delta vertical succession. A) shorezone facies succession. B) Wave dominated delta facies succession. (Modified from Clifton 2006, Bhattacharya and Walker 1991)

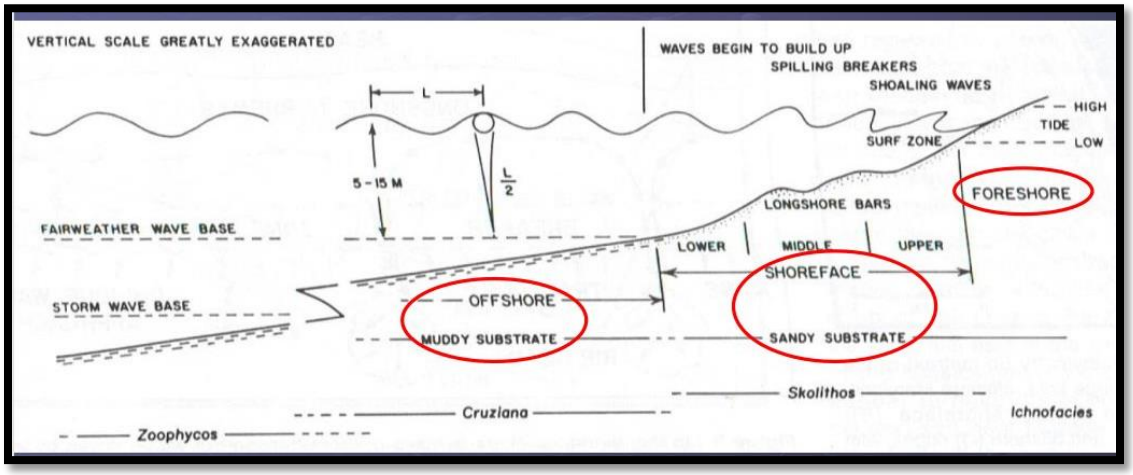

Figure 17: Typical shorezone profile. Red circles mark the principal environments and their facies. (Walker and Plint, 1992)

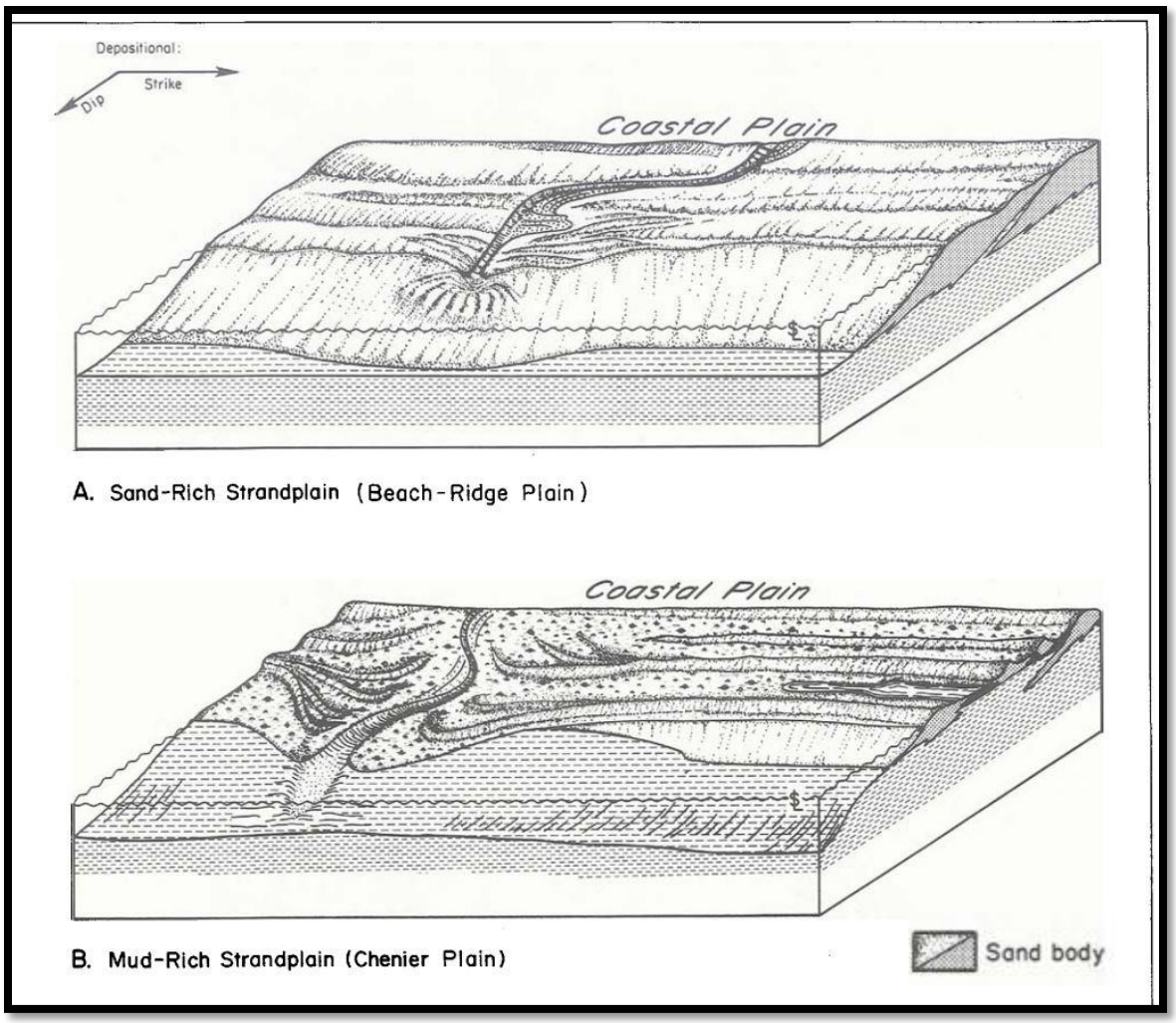

Figure 18: Illustrative models showing the typical strandplain environments of deposition. (Galloway and Cheng, 1985 in Ambrose. and Tyler, 1985)

INCISED VALLEYS

During relative sea level fall, the scouring ability of fluvial systems creates down cutting valleys. Rapid fall below the shelf margin commonly creates canyons; these valleys are assumed to be possible medium of sediment transport to the basin (Vail et al. 1984). Incised valleys can be differentiated from channels in terms of size and geometry; channels are usually smaller than and not as wide as incised valleys (Gibling, 2006).

Sediment fill of the valleys usually occur during sediment retrogradation and also through fluvial deposits prograding even during a sea level rise (Zaitlin et al., 1994). The facies differ between the fluvial influenced deposits and the marine flooding deposits, classically with coarser sand at the base overlain with sediments in an upwarding fining trend in the river filled valleys and the marine filled valleys containing structure-less muddy sediments and poorly sorted sands (Figure 19). Nevertheless, an incised valley fill may represent sediments derived from both marine and river environments (Figure 20)

An incised valley system can be subjected to multiple episodes of cuts and fills (Figure 21), this creates a complex or compound incised valley system (Zaitlin et al., 1994). Within these systems, parasequence sets exist; this usually creates challenges in chronostratigraphic grouping of sediments. The age defining boundaries such as maximum flooding surfaces and sequence boundaries are usually obscured.

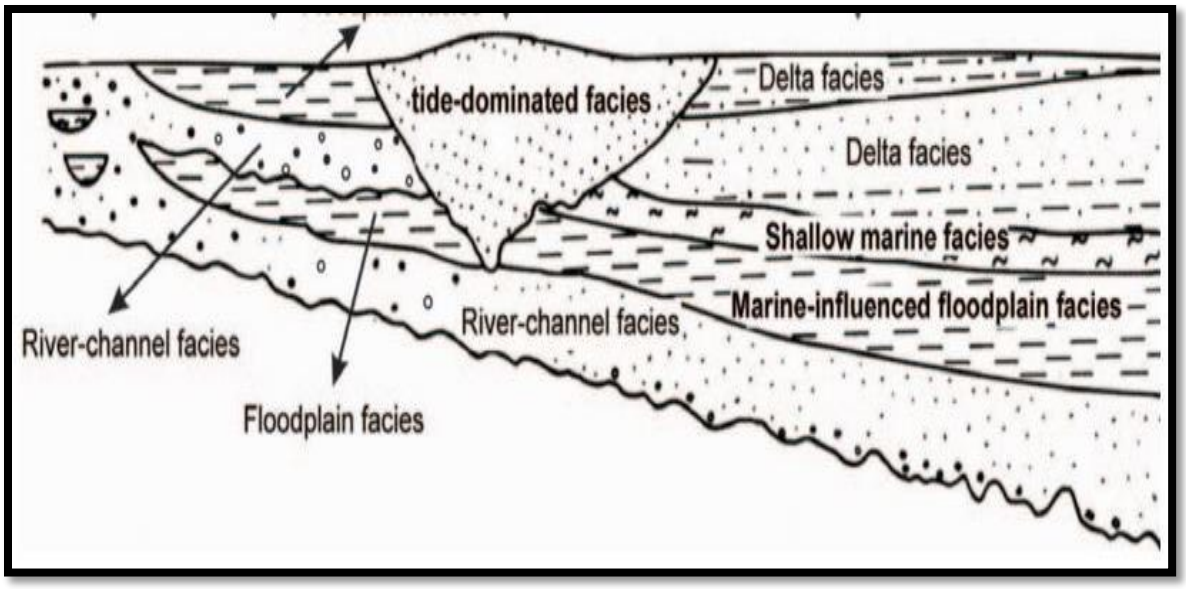

Figure 19: Longitudinal profile of facies distribution in an incised valley. (Congxian et al., 2006)

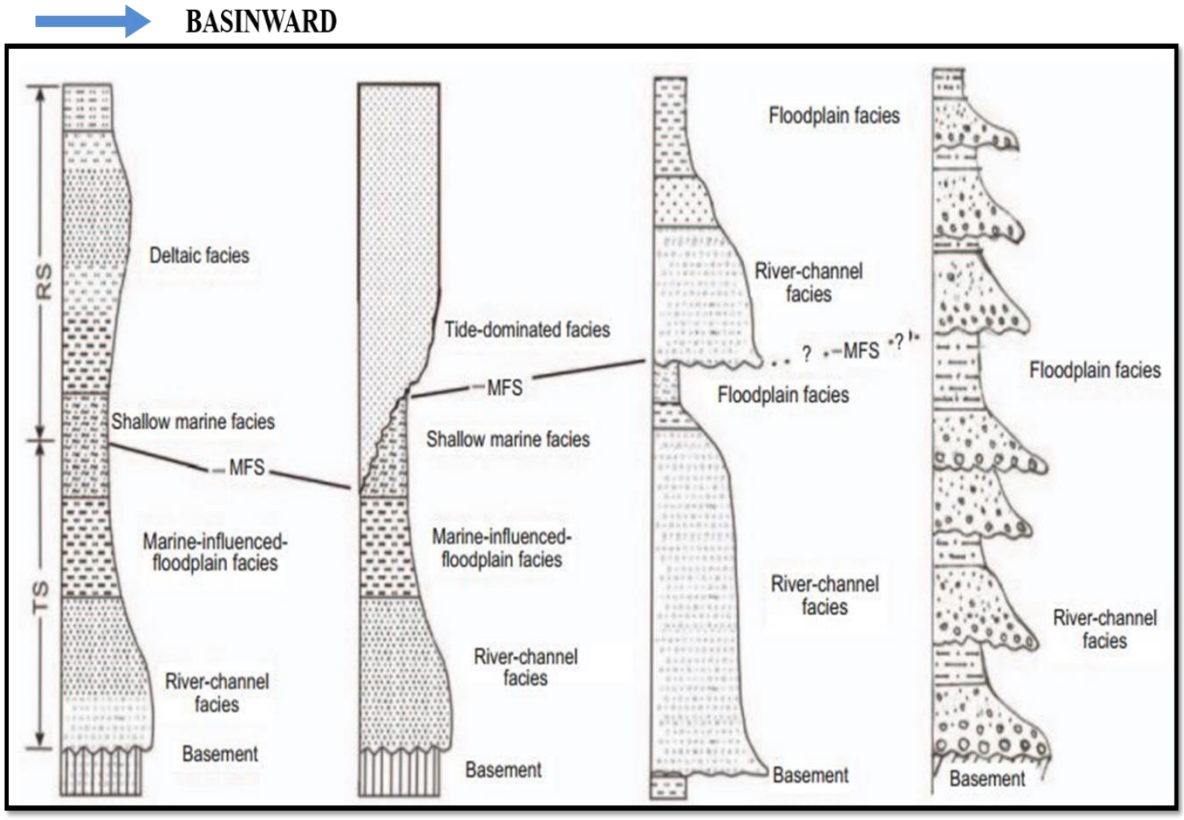

Figure 20: Facies sucession types within incised valley systems. (Congxian et al., 2006)

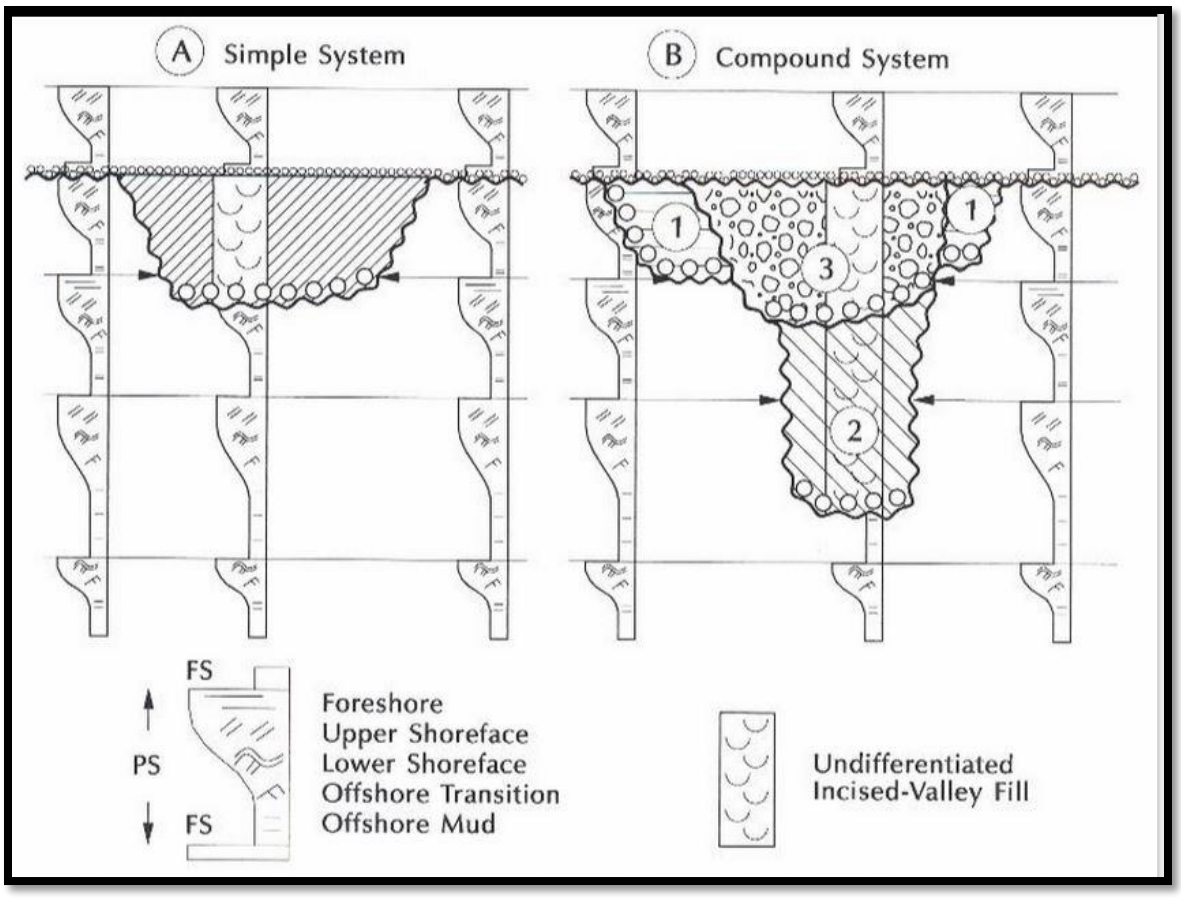

Figure 21: Schematic illustration of (A) simple and (B) compound incised-valley systems. Numbers 1-3 refer to successive episodes of cutting and filling within the incised valley. PS= parasequence; FS = flooding surface. (Zaitlin et al. 1994)

ESTUARY

During transgression, sediments back-stepping will sink into valleys created during the sea falling stage. The submerged valley deposit is referred to as an estuary; depending on the prevailing marine conditions, an estuary will be tide dominated or wave dominated. Estuaries represent a transition zone between marine and fluvial environments (Figure 22) and thus, receive sediments from both sources (Dalrymple, 2006)

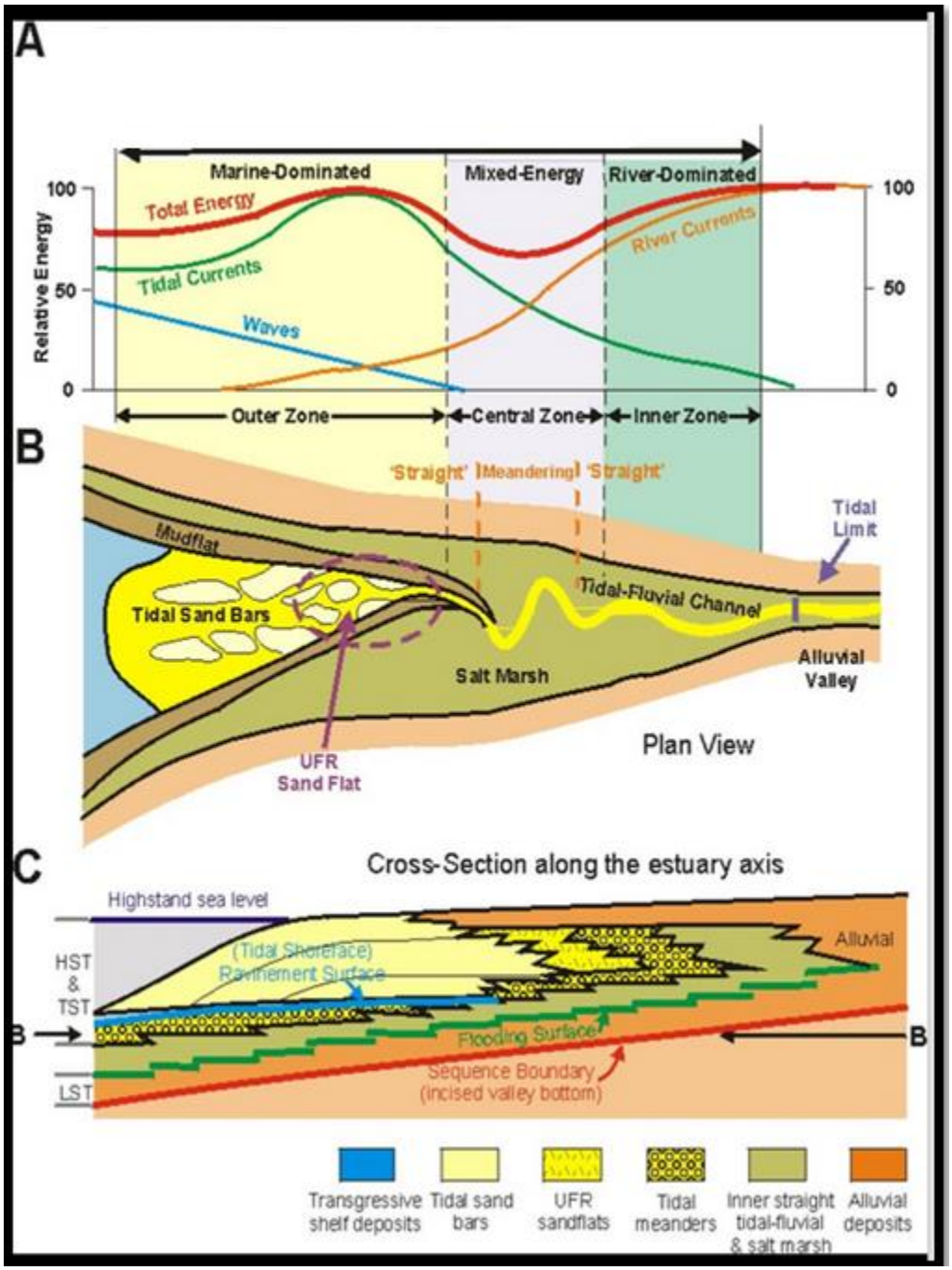

Figure 22: An illustration of a typical estuary environment. A) An estuary is influenced by both marine and fluvial environments. B) The resultant depositional environment with fluvial derived channels and marine influenced sand bars. C) Estuaries contain heterogeneous deposits from two sources. (Dalrymple et al. 1992 in Olariu 2014)

WELL-LOG REFLCTIONS IN DEPOSITIONAL ENVIRONMENTS

Well logs provide useful information that aid sedimentary basins investigations. The lithology logs- gamma ray, spontaneous potential were employed in this study. In a shale dominated zone, the spontaneous potential log deflects towards zero; shale is a low porosity and relatively impermeable rock type.

The gamma ray lies along the left-hand side of the log (Figure 23), it measures natural gamma radiation in the rock and records high values at such intervals. The spontaneous potential also lies along the left-hand side of the log; it estimates the permeability of the rock. I observed that some areas showing presence of sand on the gamma log pattern appeared nil on the spontaneous potential logs, the electro chemical contrast between the bore-hole and rock fluids may not be significant (Galloway and Hobday 1983). For example, deeper formations typically have more saline waters than well log fluids; this disparity yields a leftward curve log response within porous and permeable intervals. Sand intercalated with mud could have low porosity and permeability, thus gamma ray logs were used mostly and spontaneous potential logs were used in their absence. Spontaneous potential logs are also sensitive to the presence of hydrocarbon (Figure 23), and it will record reading in intervals where the pore space is filled with hydrocarbon (Torres-Verdin 2010).

Wireline log signatures have been successfully used to define depositional cycles in the Cenozoic GOM (Van Wagoner et al. 1990, Robert G. Loucks et al. 2011, Brown et al. 2005, Fongngern and Ambrose 2012). Though they used the gathered information from the well logs in combination with other data to build sequence stratigraphic models for

their specific studied sections, certain general depositional styles for strata of the Cenozoic GOM have been established.

Deltas

Deltas typically showcase an upward coarsening well-log pattern (Bhattacharya and Walker 1991). They are bounded on top by a significant transgressive surface referred to as maximum flooding surface (MFS); MFS is a stratigraphic surface that represents the end of retrogradation of marine sediments (Figure 24). Following this surface is typically progradation of highstand (high sea level) deltaic sediments (Figure 25). Wave dominated deltas show a blockier pattern, this indicates less mud present.

Shorezone

Shoreface and strandplain/beach environments typically consist of massive sand deposits, and hence portray a blocky, but overall upward coarsening pattern. These characteristics are similar to a wave dominated delta; they can be differentiated by the sharp basal contact with the underlying mud deposits observed in shoreface deposits (Figure 26).

Incised valleys

Incised valley fills record multiple facies usually with a basinward shift in facies at the base (Figure 27). Well log records a sharp base and blocky aggradational sand body, overlain by an upward fining trending sedimentation. Typically, estuaries are part of incised valleys fills.

Estuaries

Estuaries generally exhibit an upward fining well log trend (Figure 28). The basal component is usually marine derived sand bodies, which has been interpreted as bay-head deltaic sediments. This delta is smallest of deltas, during sea level rise, the delta is moved back into an incised valley; forming the early part of transgressive deposits (Dalrymple et al 1992).

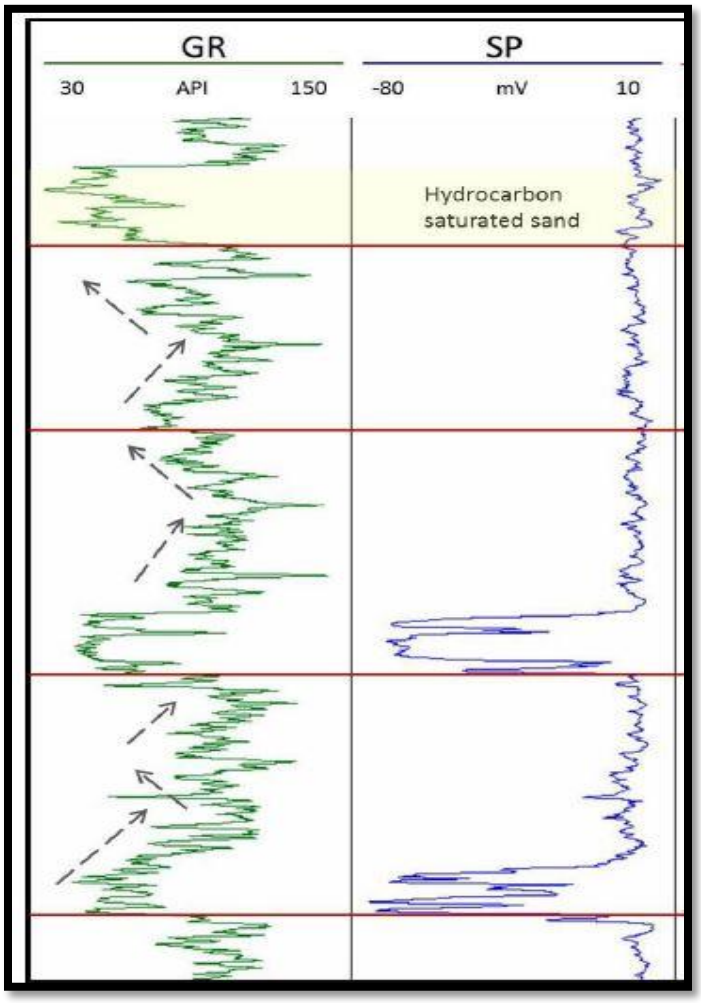

Figure 23: An example of gamma ray and spontaneous potential logs. Note the difference in response between both logs in the sand-shale intervals and also in the hydrocarbon saturated zone. (Fongngern 2011)

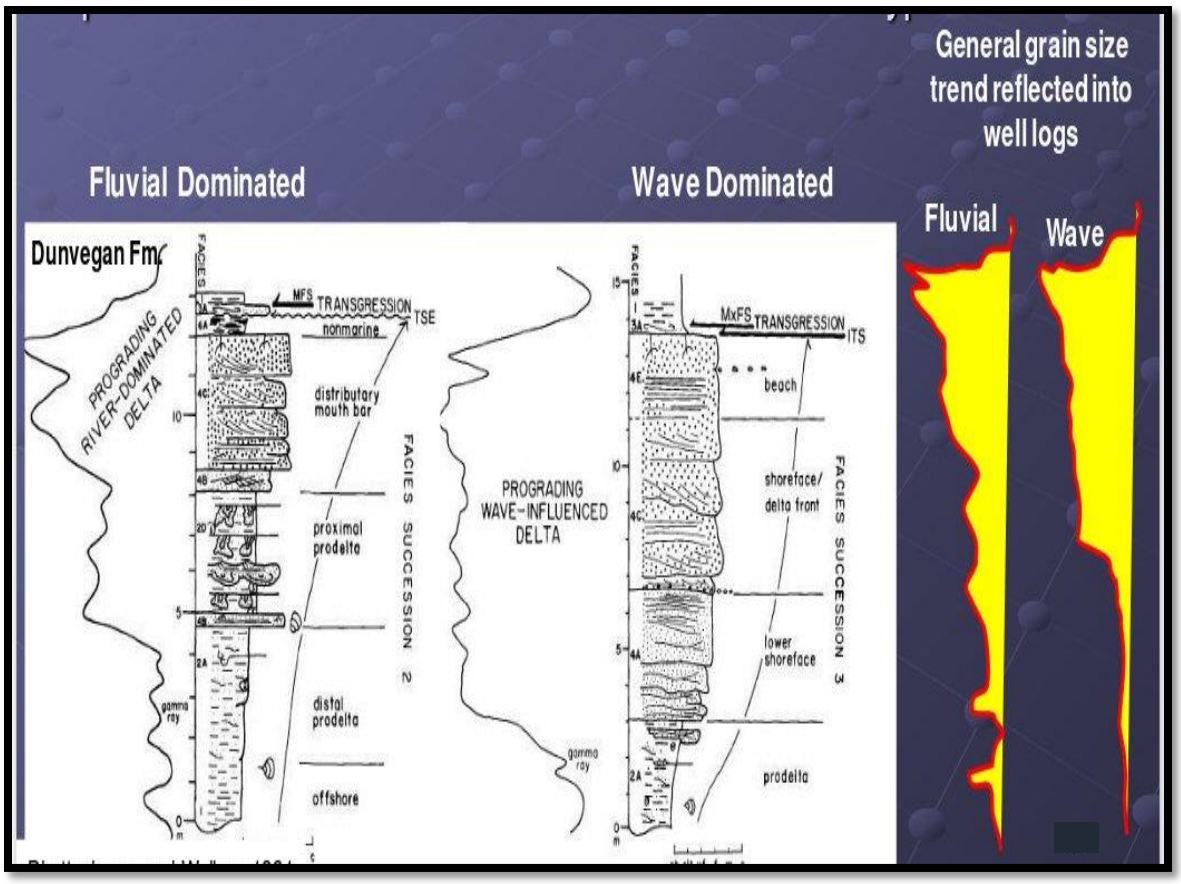

Figure 24: Typical well log response in fluvial and wave delta environments. Deposits are overlain by MFS. (Bhattacharya and Walker 1991 in Olariu 2014)

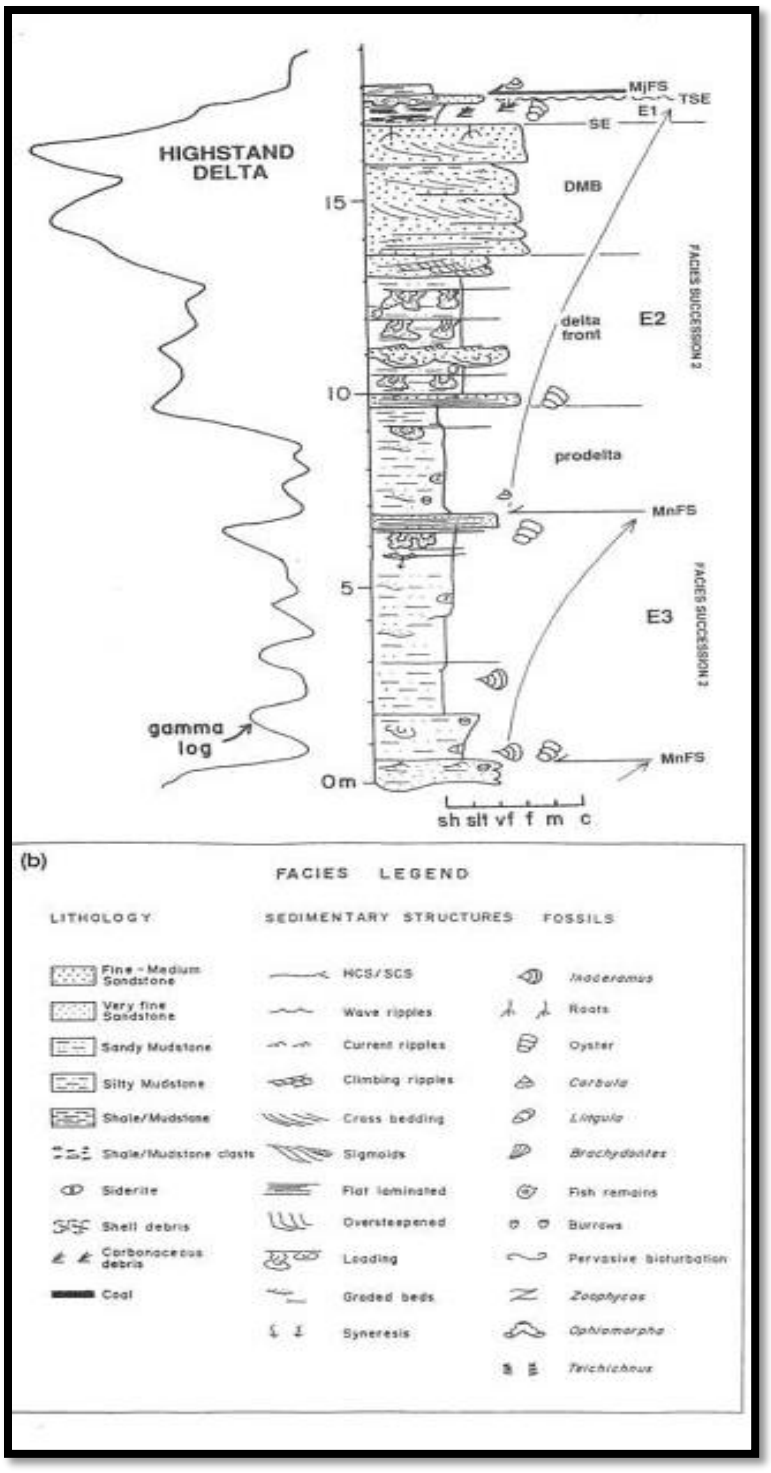

Figure 25: Highstand delta well log pattern. (Bhattacharya and Walker 1991)

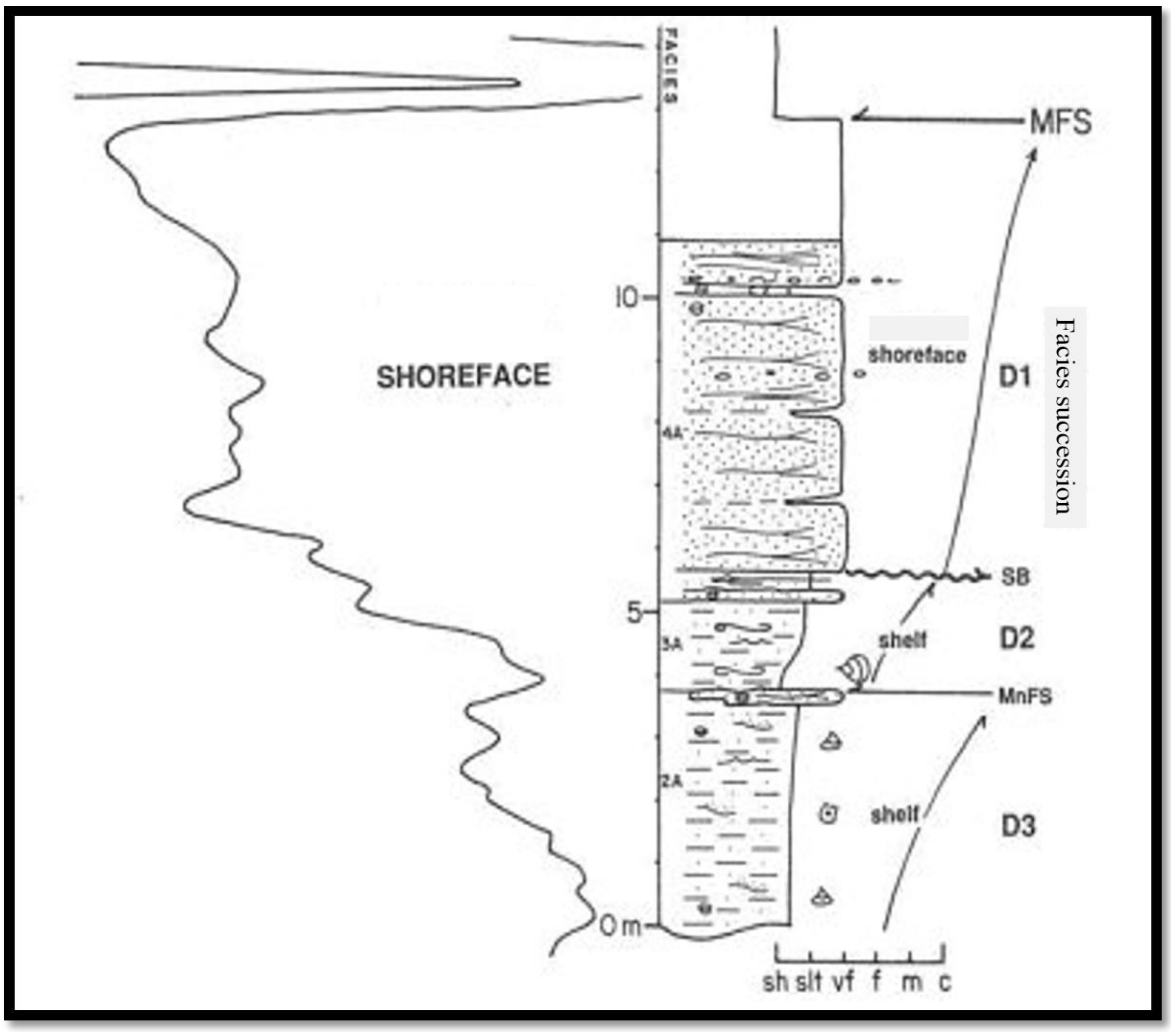

Figure 26: Well log through a shoreface environment. (Modified from Bhattacharya and Walker 1991)

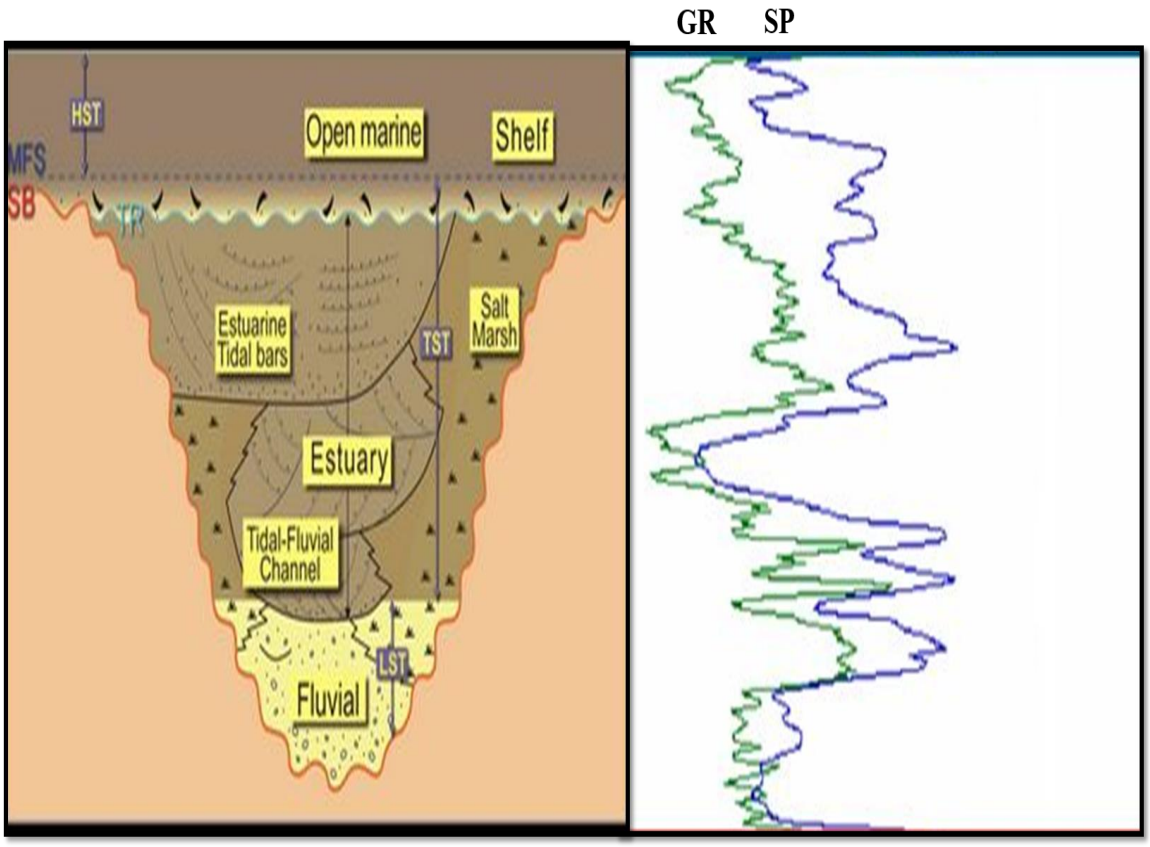

Figure 27: Typical dip section of incised valley fill and well log pattern. (Modified from Allen and Posamentier, 1993 in Olariu 2014 and Fongngern 2011).

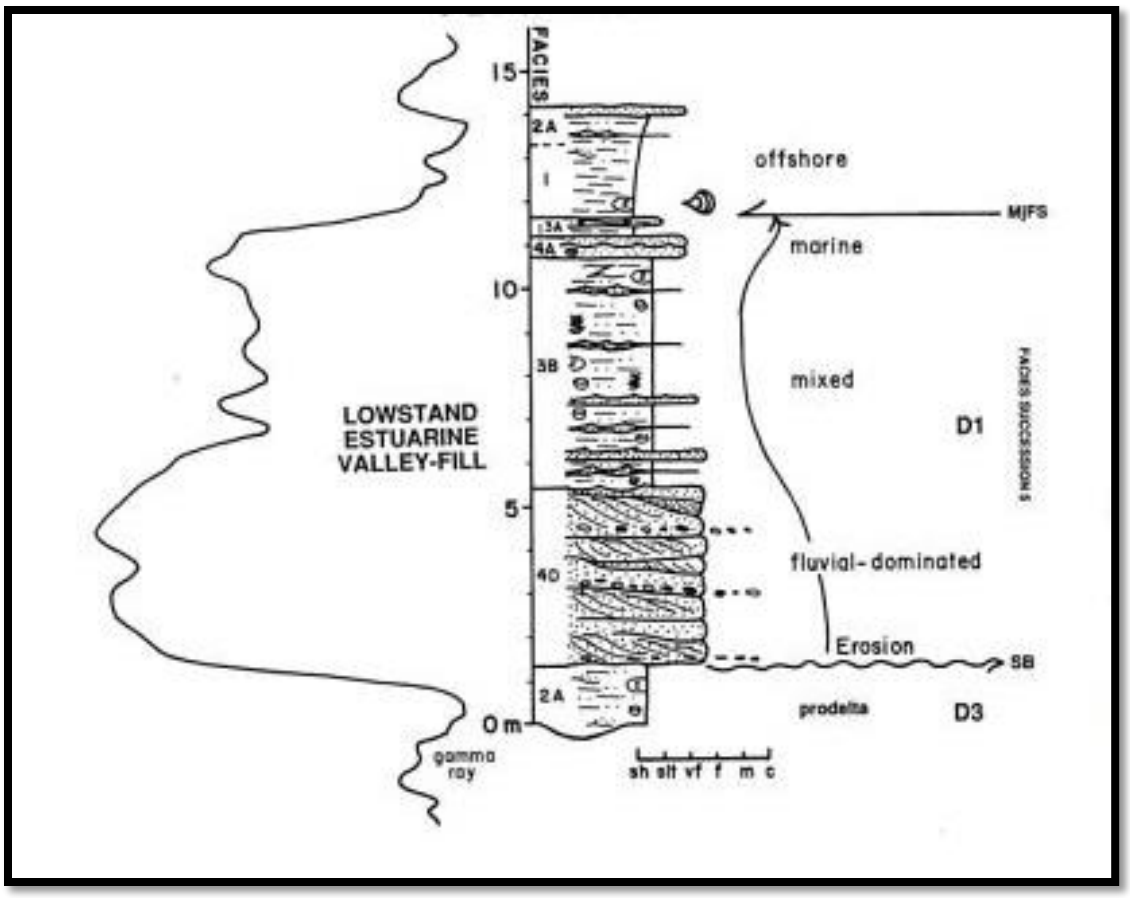

Figure 28: Well log pattern in an estuarine depositional environment. (Bhattacharya 1993)

RESULTS

Seismic attributes have their different uses and limitations. RMS amplitude attribute extraction and spectral decomposition results from regular seismic volume produced maps that did not resolve the plan-form geometries within the Lower Miocene stratigraphy and therefore were not further used in my analyses. The poor resolution of these maps may be due to relatively small impedance differences between various types of sedimentary deposits - that is, channel fill and over bank facies are not significantly different.

On the other hand, the variance maps generated from the spectral decomposition tool did reveal structures. The revelation of structures by the variance was made possible because the variance is an edge-detection attribute that identifies lateral discontinuities within the seismic volume. However, the imaged structural and stratigraphic features are better defined on the variance attribute maps obtained using the regular amplitude extraction software. Figures 29 and 30 show maps generated from the other seismic attribute volumes.

The variance attribute map generated from H1 does not show any interpretable structures (Figure 31). The H3 interval showcases well logs with upward coarsening to blocky pattern of sand (Figure 32). The sand has a thickness range 209ft to 506ft. The variance-amplitude map within this interval displays a strike oriented depositional pattern (Figure 33) of aggrading and prograding beach ridges. Isochronal map of the interval (Figure 34), revealed laterally alternating sand thicknesses. The net sand isopach map generated from sand count for the between interval H2 and H3, also depicts this thickness trend. (Figure 35).

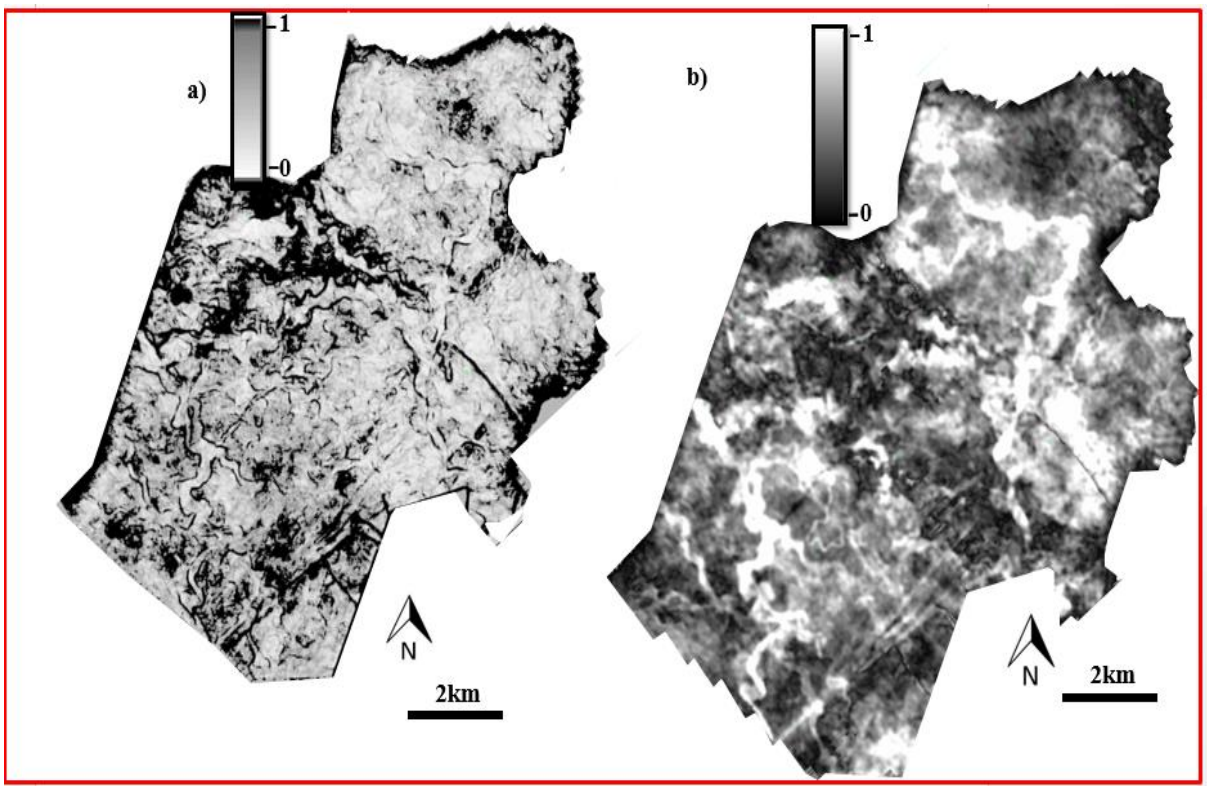

Figure 29: seismic attribute comparison maps for H7, a) is a spectral decomposed map generated using the variance volume .b) is spectral decomposed map generated using the seismic volume. For corresponding variance attribute map, see figure 38a. The channels are more visible in a. Both maps are at a frequency of 25 Hz.

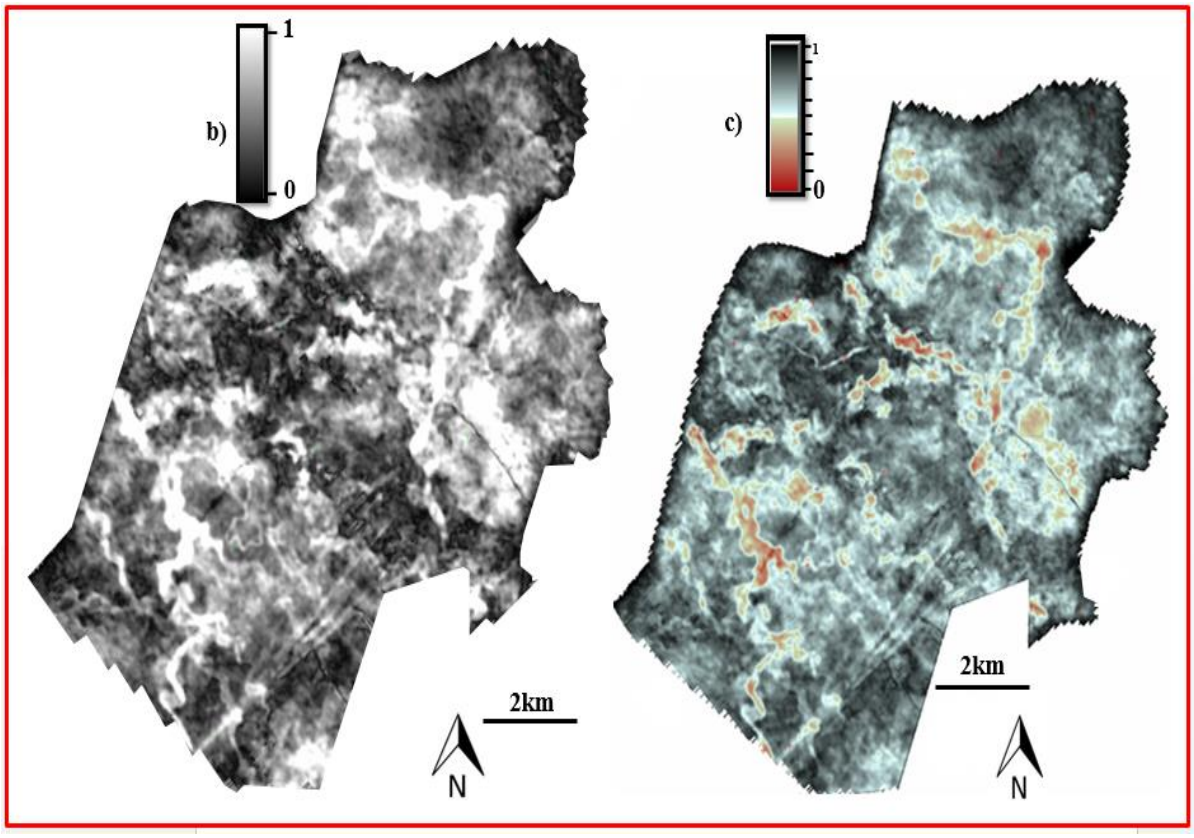

Figure 30: seismic attribute comparison maps for H7, b) is a spectral decomposed map at a frequency of 25Hz generated using the seismic volume. c) RMS amplitude map. The channels are more visible in a. Note that the channels are more visible in a, than in b, and features in b are more visible than in c. For corresponding variance attribute map, see figure 38a.

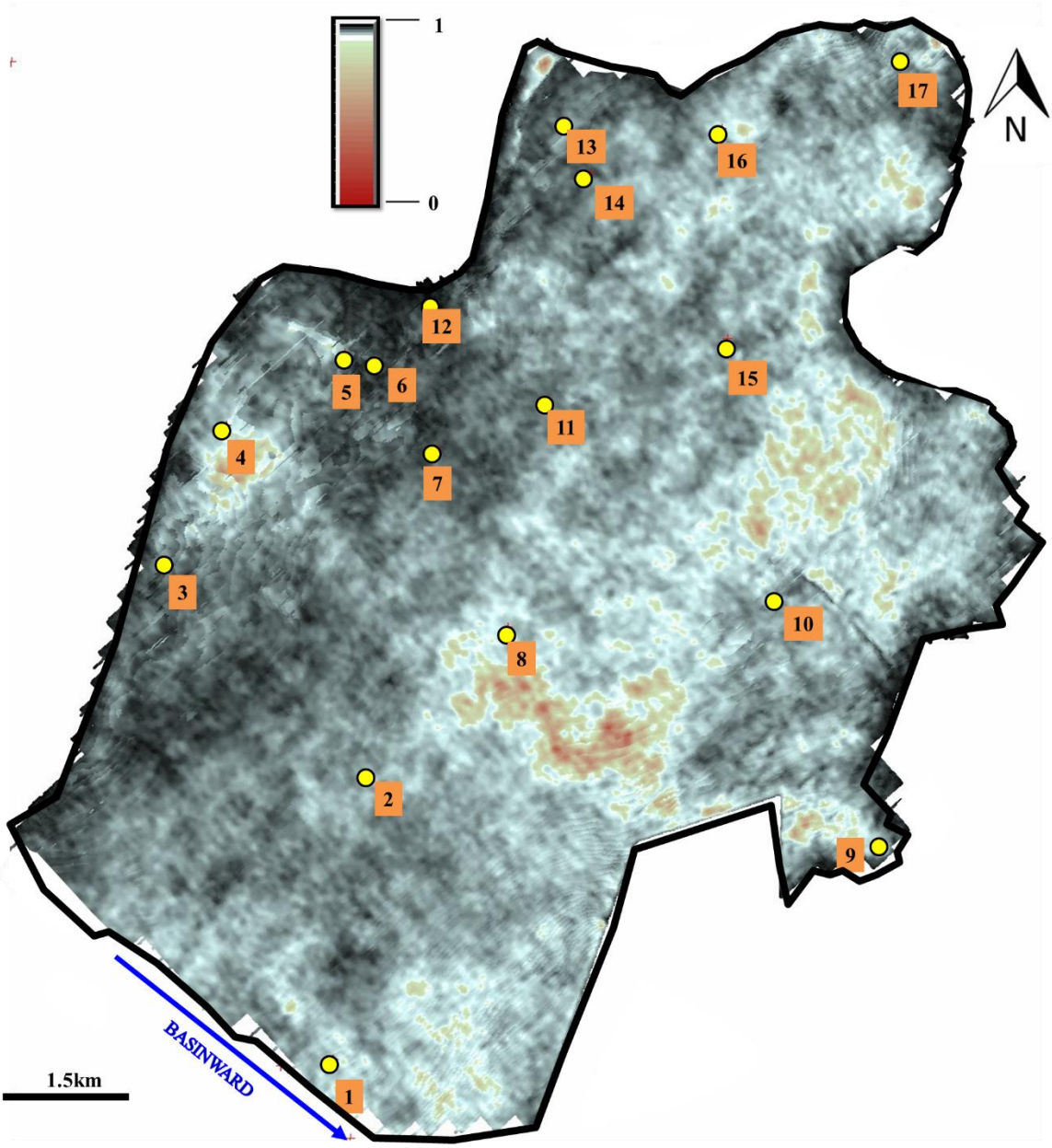

Figure 31: Amplitude-variance map for H2; Anahuac shale interval. See figure 10 for horizons positions

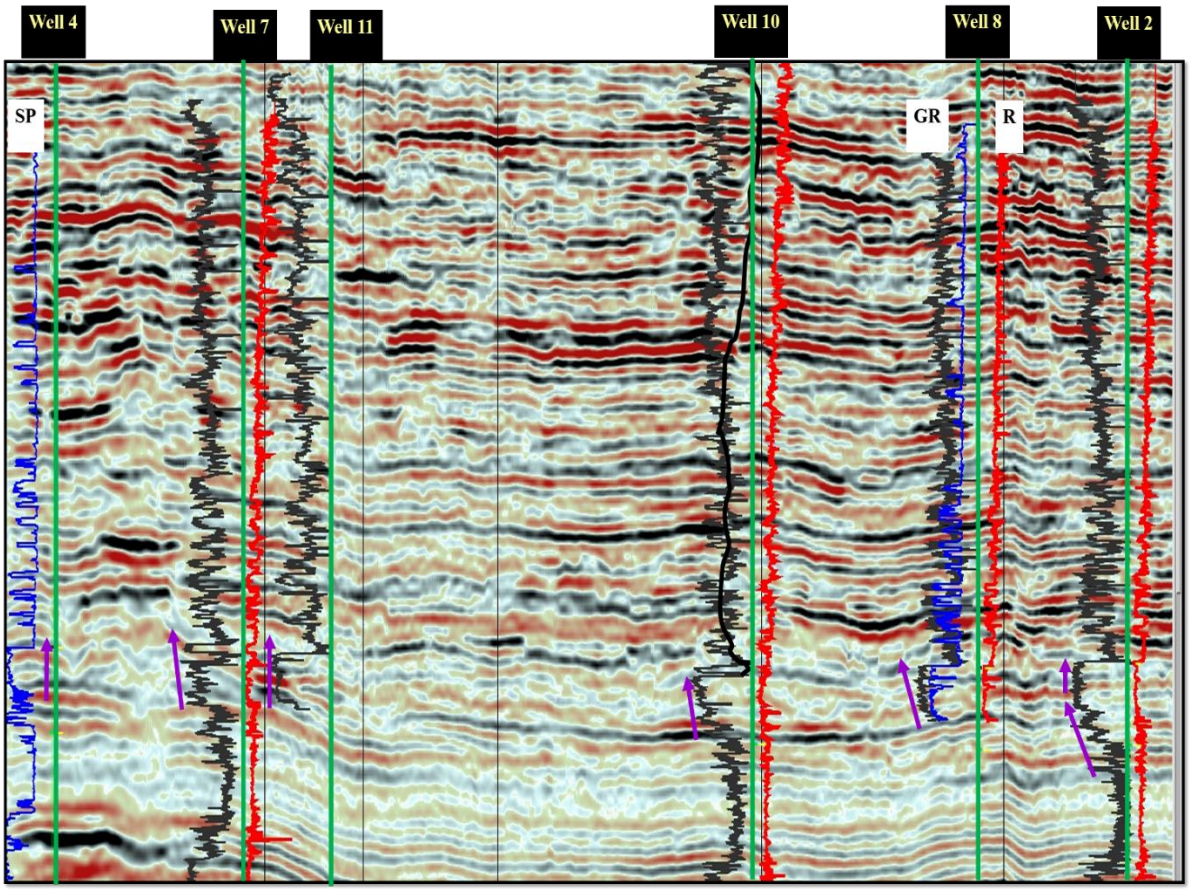

Figure 32: Coarsening upward to blocky well log pattern observed between H2 and H3. Purple arrows highlight the well log patterns.

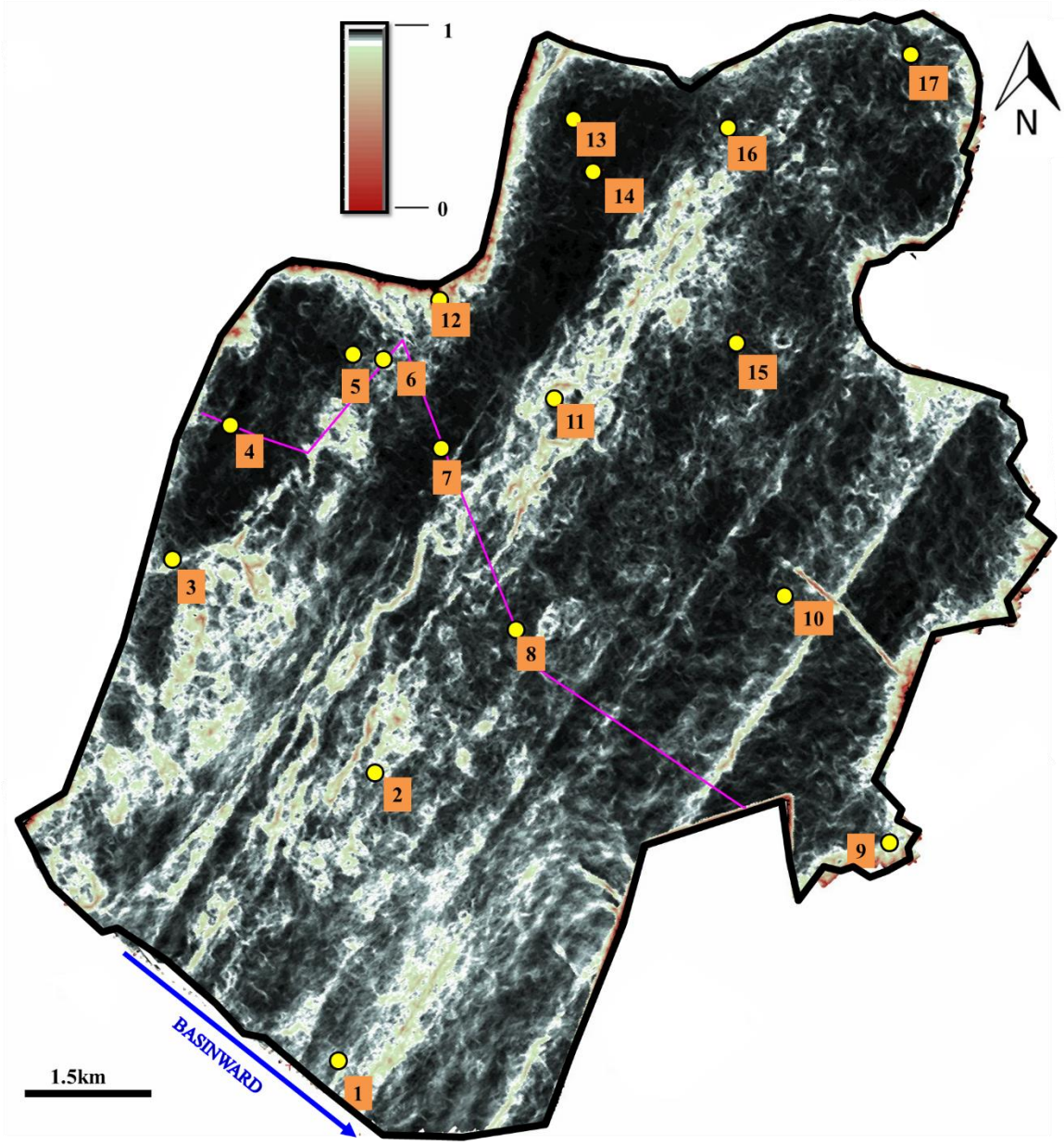

Figure 33: Amplitude-variance map of H5. Shoreline oriented deposits. Purple line indicates thickness trend shown on the isochron map.

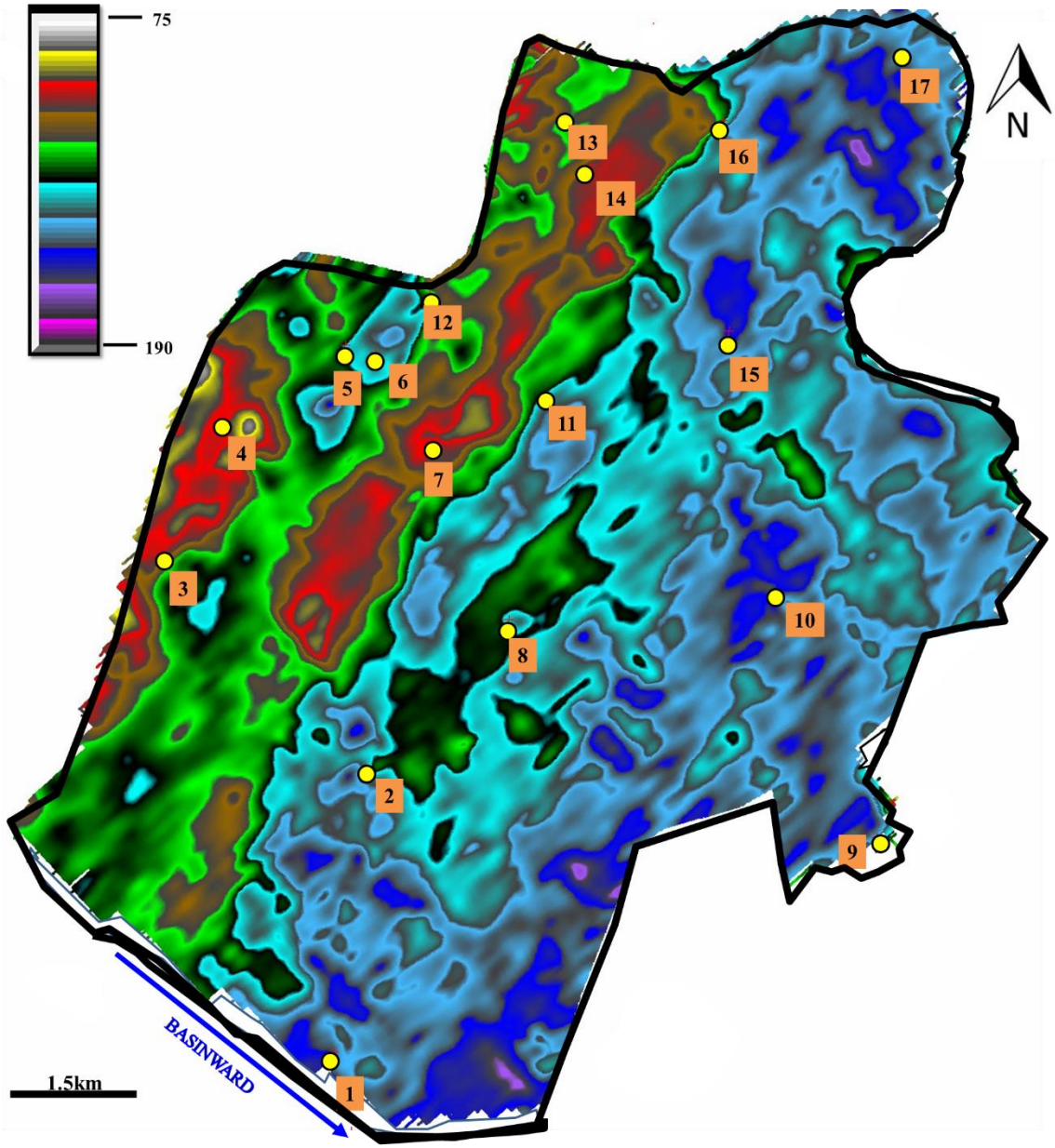

Figure 34: Isochron map between H3 and H5. Warm colors are low values, cool colors are higher values.

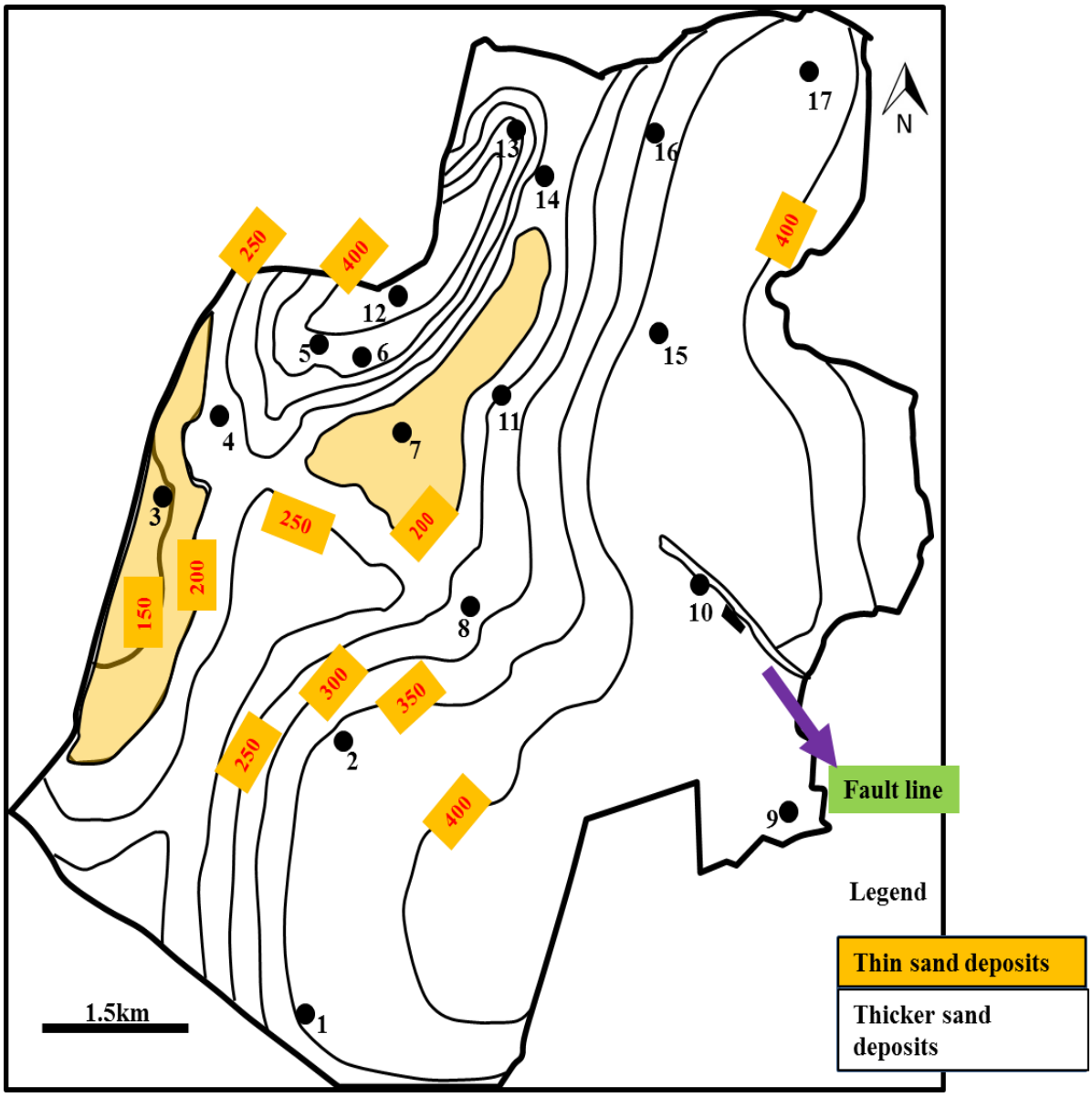

Figure 35: Net-sand isopach map between H3 and H5.

The overlying intervals from the top of H3-H6, shows a coastal plain environment consisting of deposits filling channels and channel belts with no obvious structures defining erosional valley walls (Figures 36&37). Maximum channel-belt length Maximum channel-belt length is approximately 21000ft and widths range between 330-3000ft. Well log pattern is mostly serrated, with intermittent occurrence of thick shale or sand bodies.

Abundance of channels and channel belts dominate the interval above at depth 3000ft (H7). Channels are sinuous but exhibit little lateral migration (i.e., no laterally continuous point-bar deposits). The first incised valleys observed in Lower Miocene strata are shown in Figures 38&39. Measured valley length ranges from 6360-35200ft, and widths for the erosional structures vary between 445-2300ft. Notice that these valleys also preserve remnant topographic highs within them (Figure 38). Towards the southwestern axis of this map, an under developed beach structure is exhibited. Well log at this interval exhibits an upward coarsening pattern with an extensive basal shale response.

Moving up through the volume into younger strata- H9 to H11, the dominant stratigraphic features are channels and incised valleys. The valley walls are characterized by larger scoops with more curvature that match the form of the outer banks of migrating river bends (Figures 40 &41). Well logs transecting some of these features showed presence of sands. Valley dimensions range from 2,590-3,650ft wide and 9,853 -15,000ft Long. The variance attribute maps for the youngest intervals H12 to H15 do not clearly show structures when compared to older sections (Figure 42).

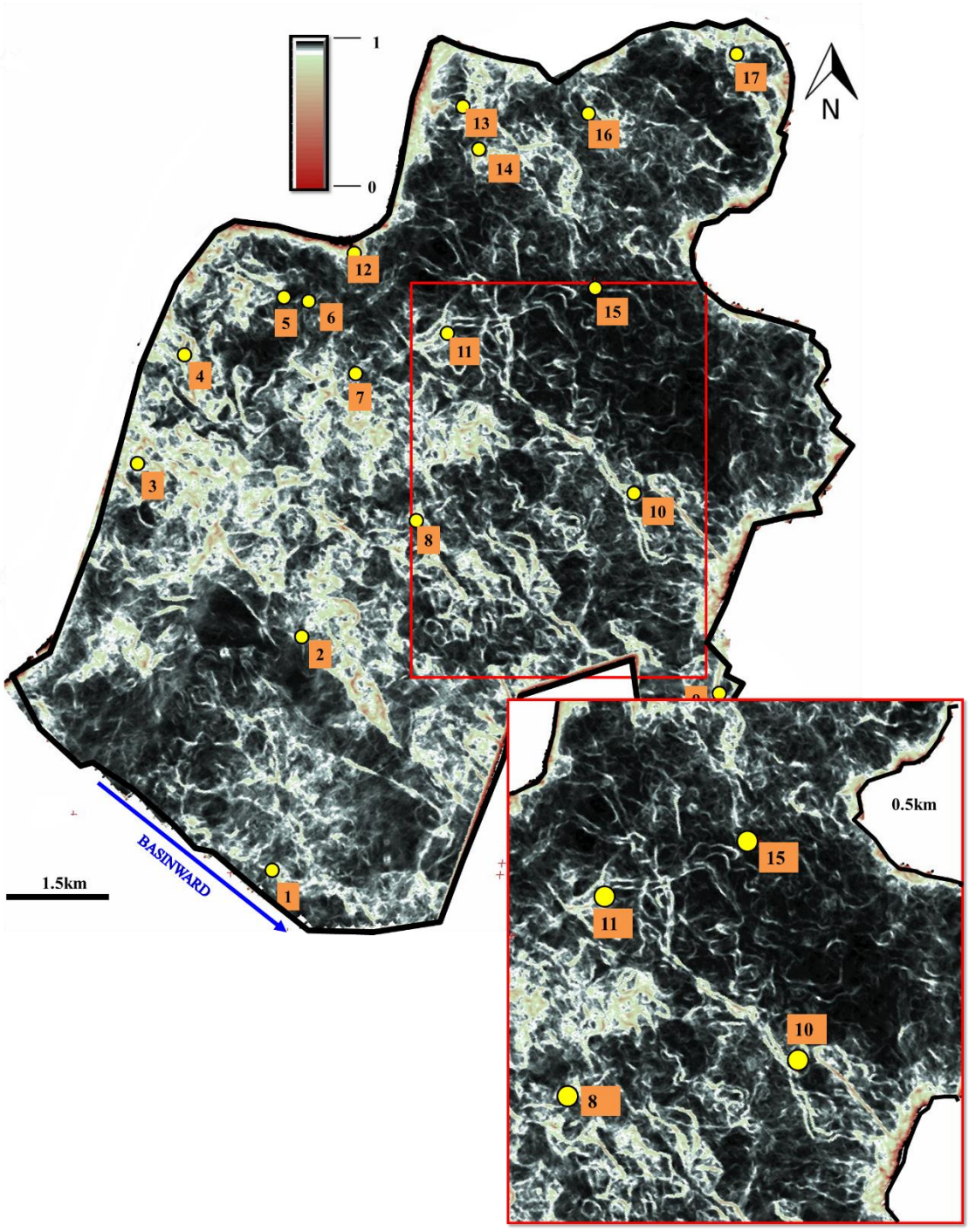

Figure 36: Variance attribute map for H4 showing first occurrence of fluvial deltaic environment..

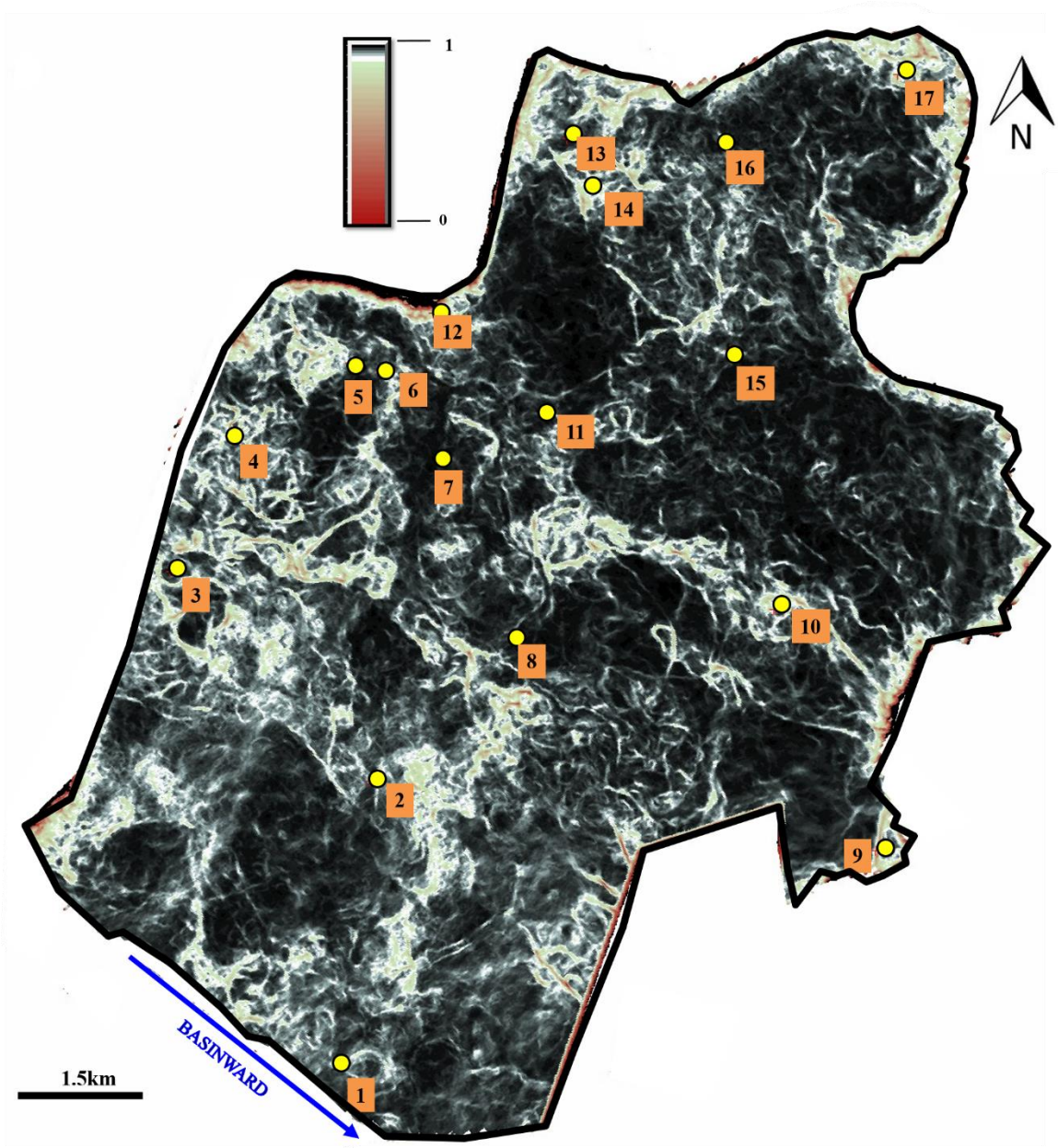

Figure 37: Variance attribute map for H5. Presence of numerous channels indicate further in-land position of the shoreline.

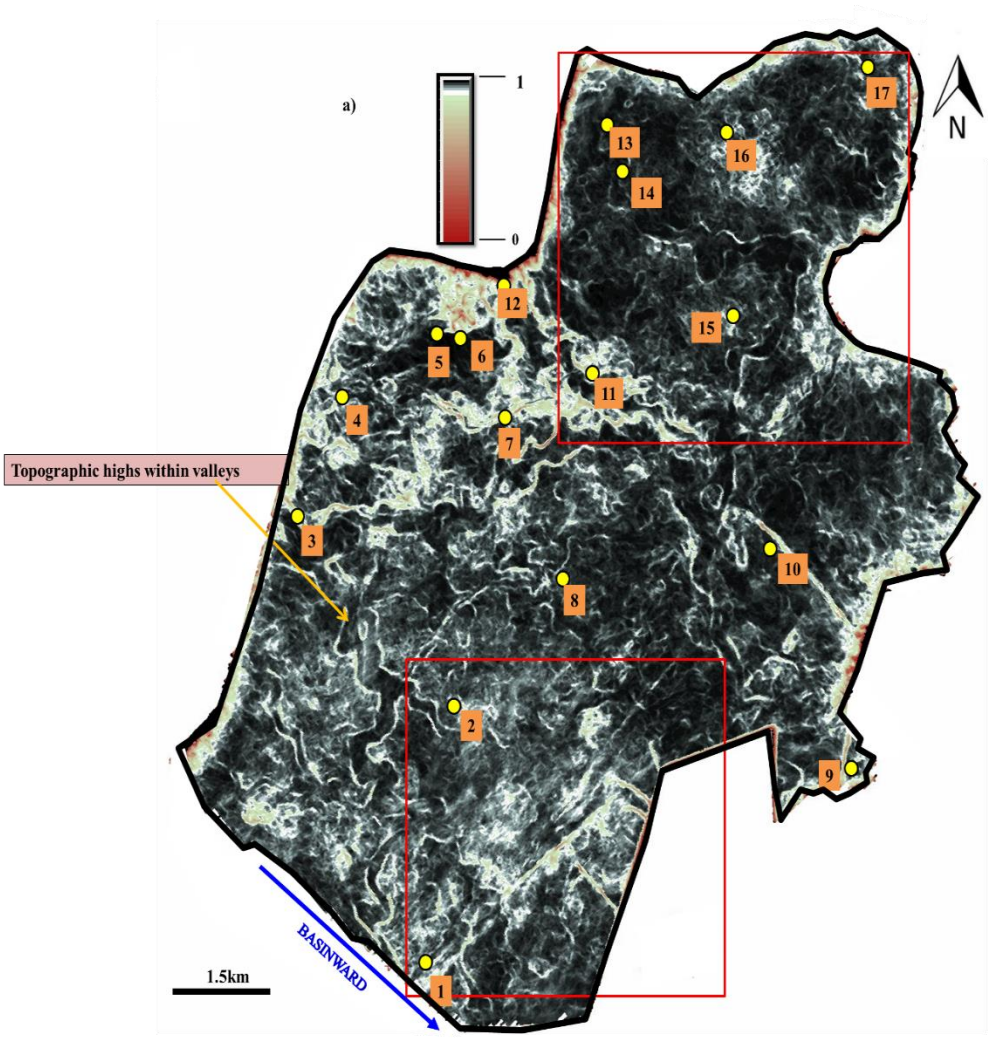

Figure 38a: a) Amplitude variance map of H7 showing sinuous channels characterized by minimal lateral migration, marked up areas in red are shown in figure 38b

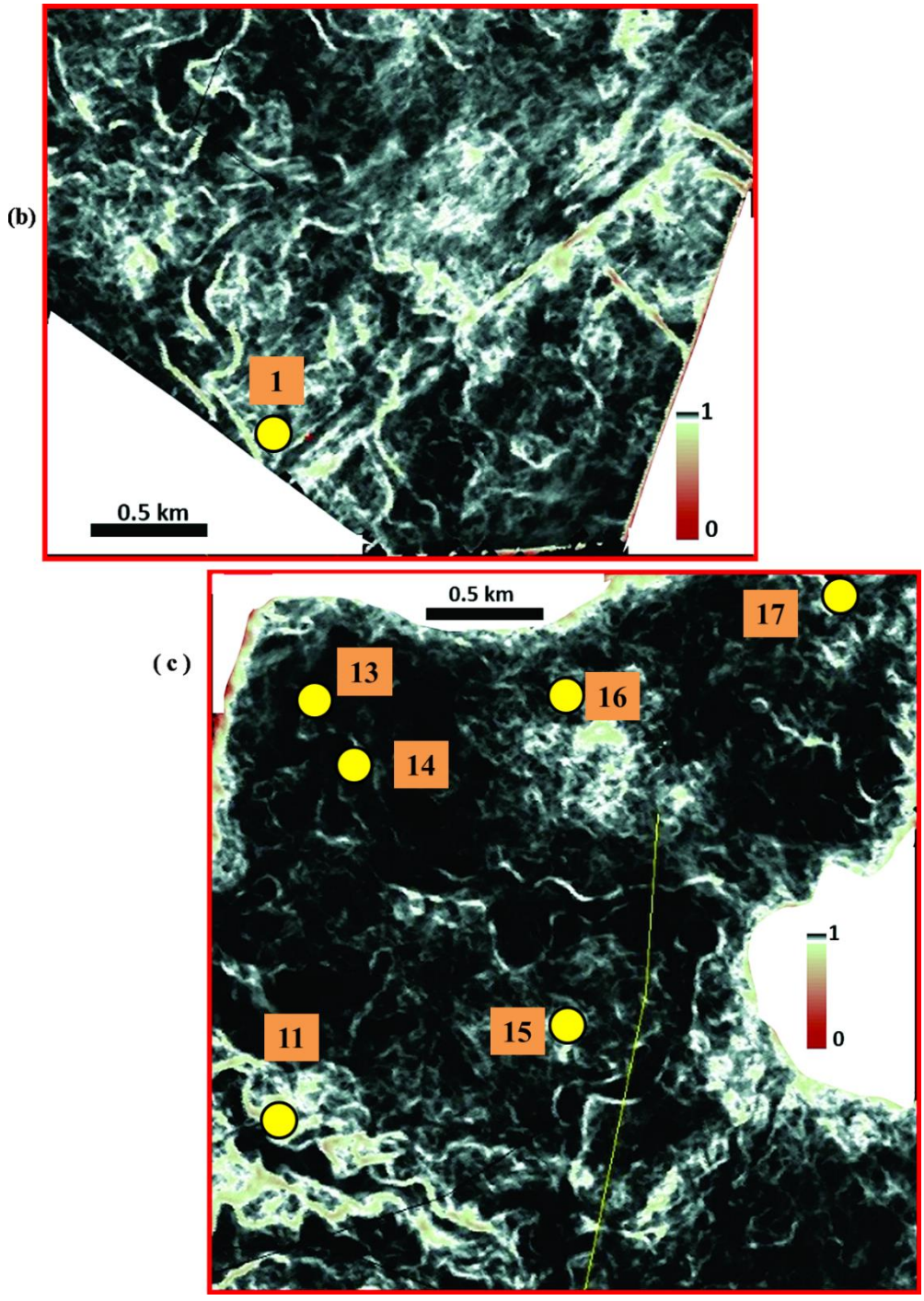

Figure 38b: b) Northeast-Southwest inclined feature of the short-lived strandplain. c) distinctive channel present in the map northern axis for H7

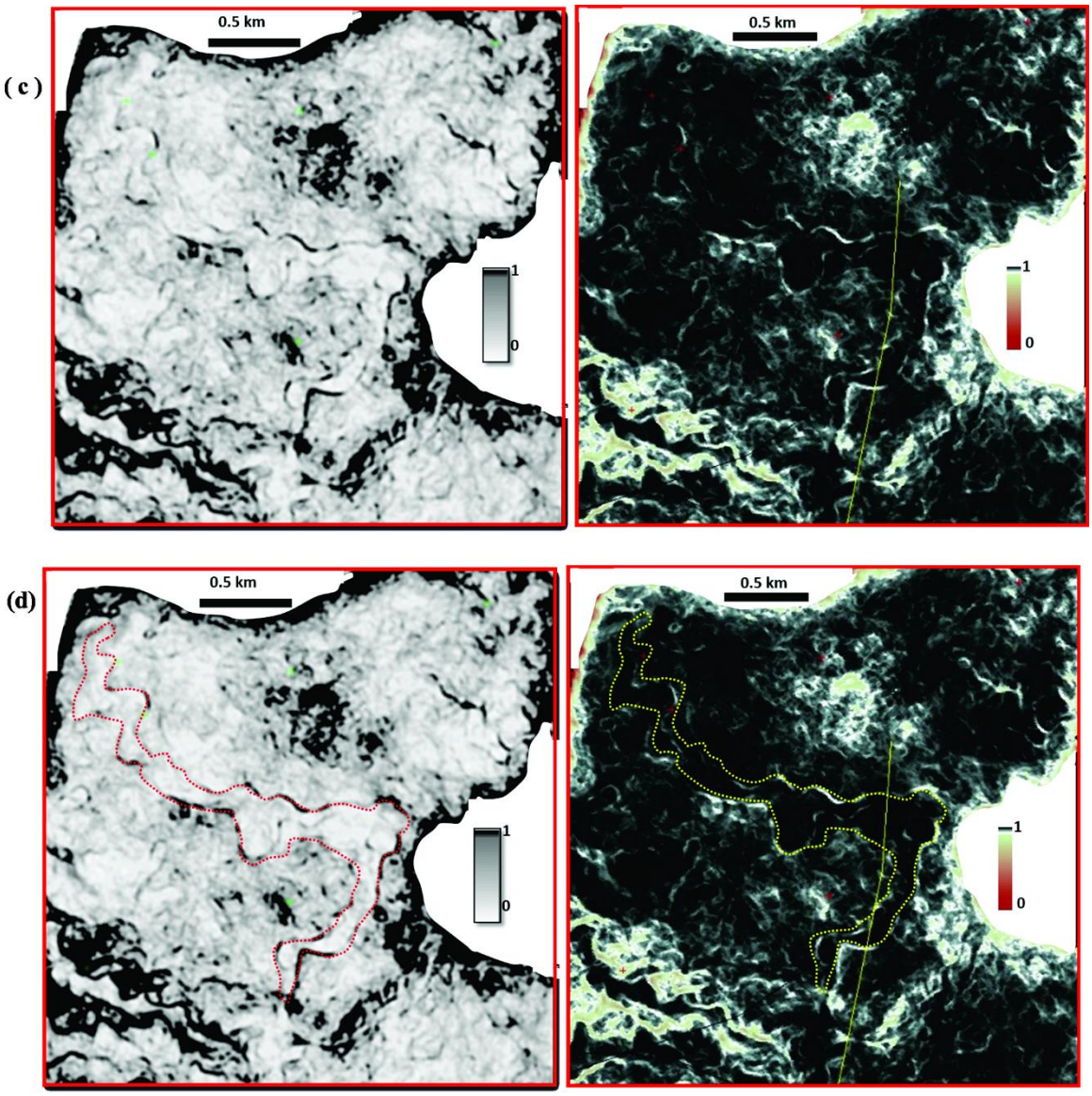

Figure 38c: Figure c shows some features are more visible in the spectral decomposed variance attribute maps. d) Figure d highlights the channel featured in c.

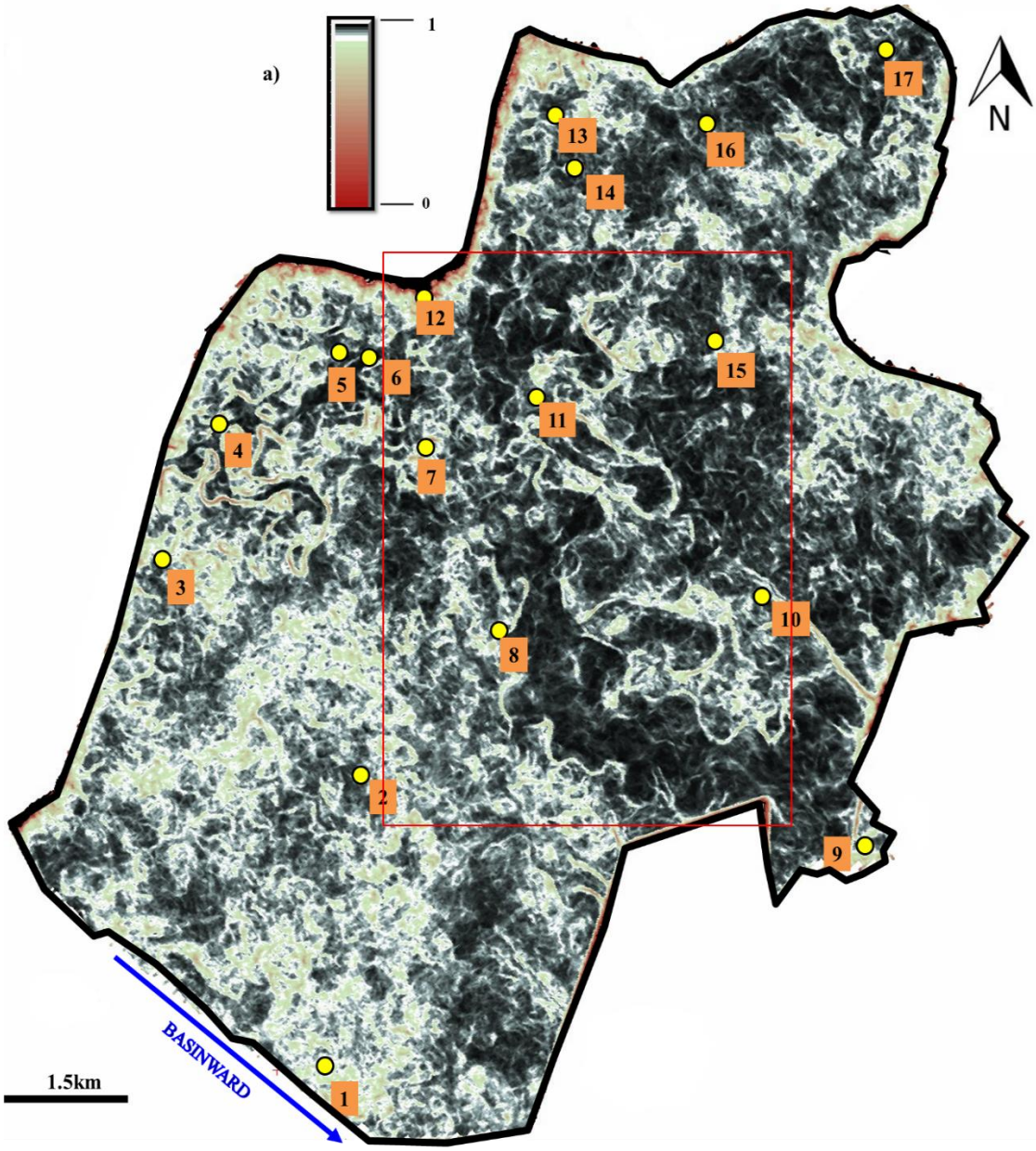

Figure 39a: Variance attribute map for H8 showing sinuous channels and valley cuts. The red marked out portion is shown in figure 39b

b)

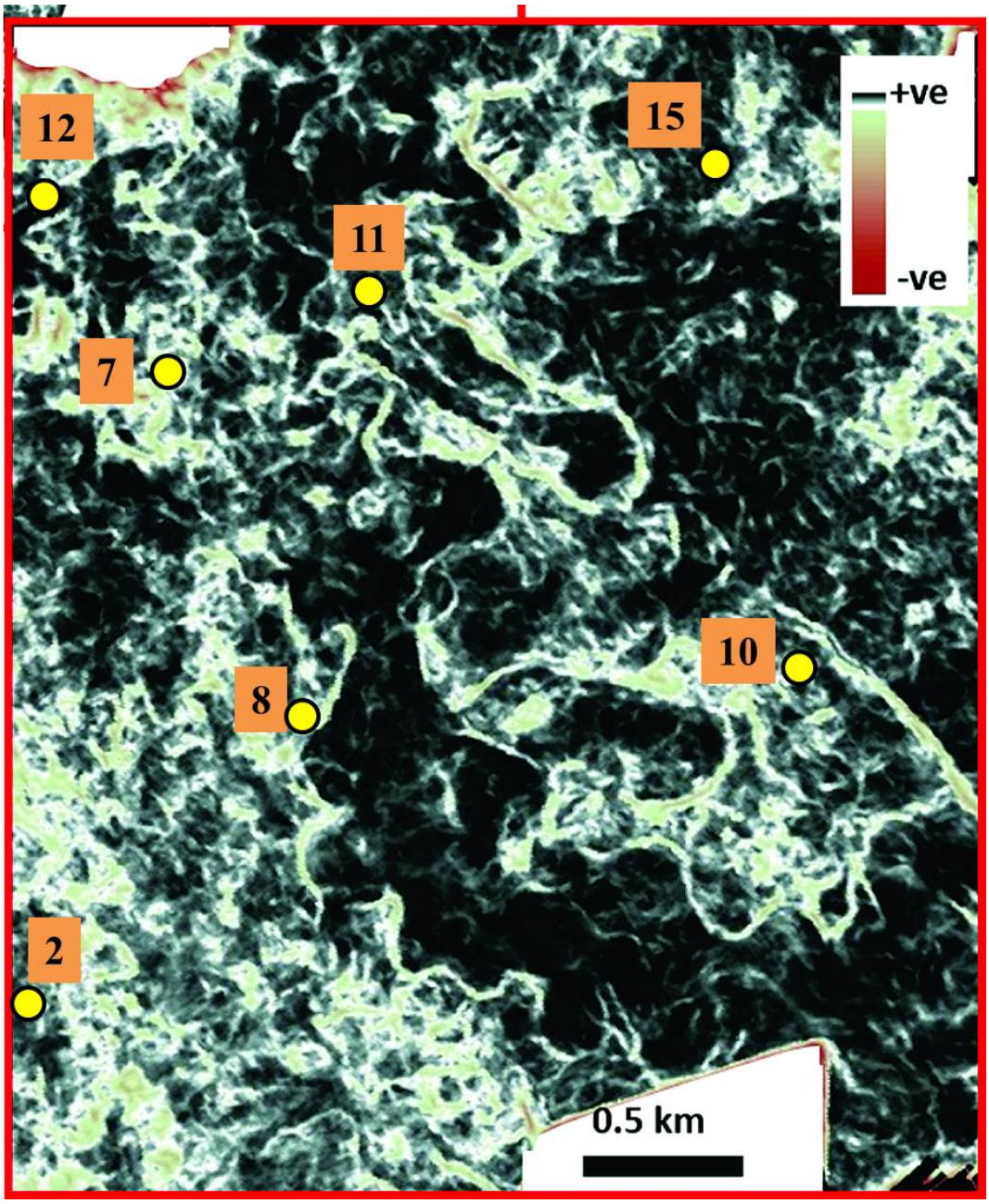

Figure 39b: Sinuous channels featured in H8 extending to the basin

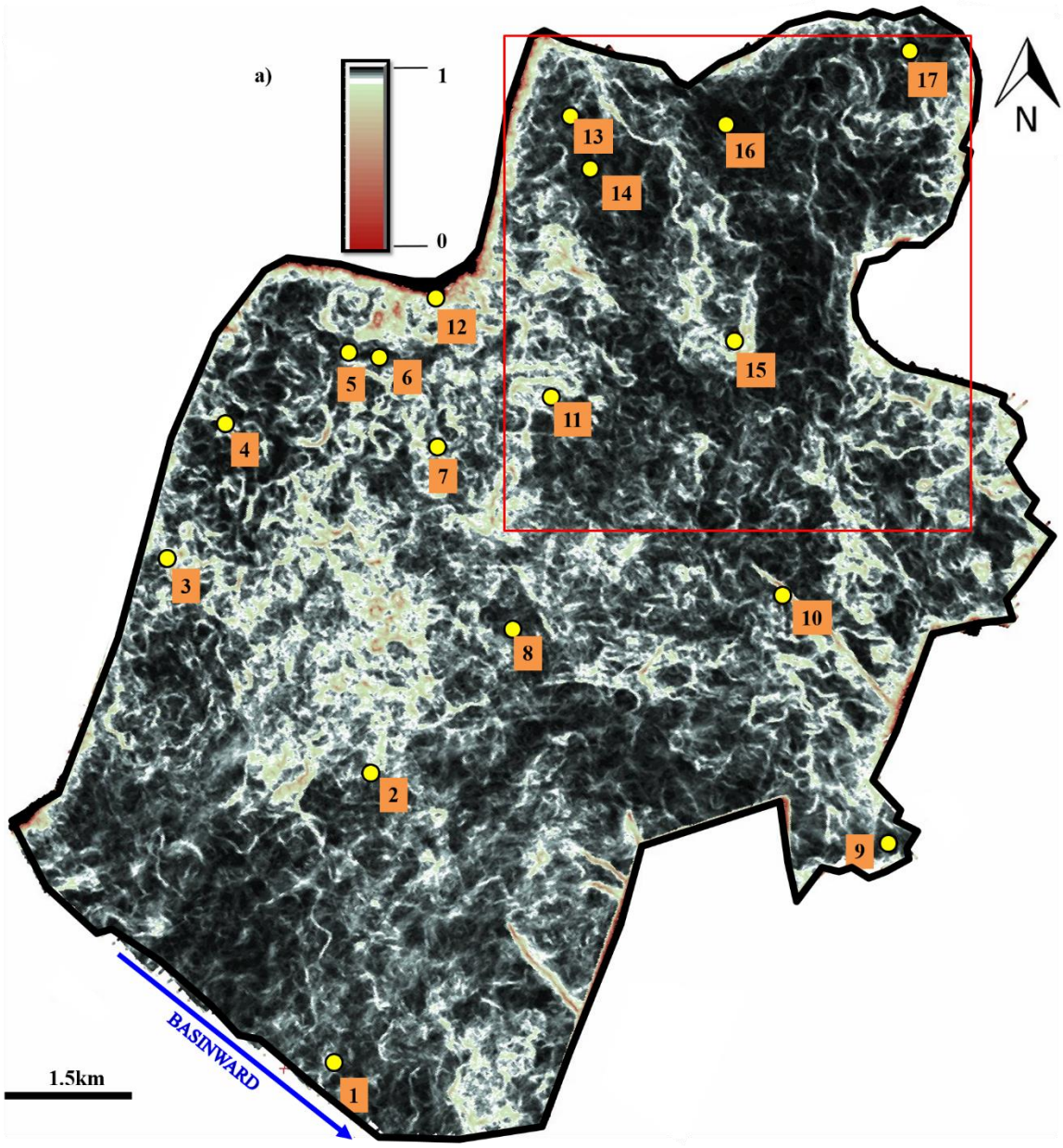

Figure 40a: Variance attribute map for H9 featuring large channels. The red marked out portion is shown in figure 40b.

b)

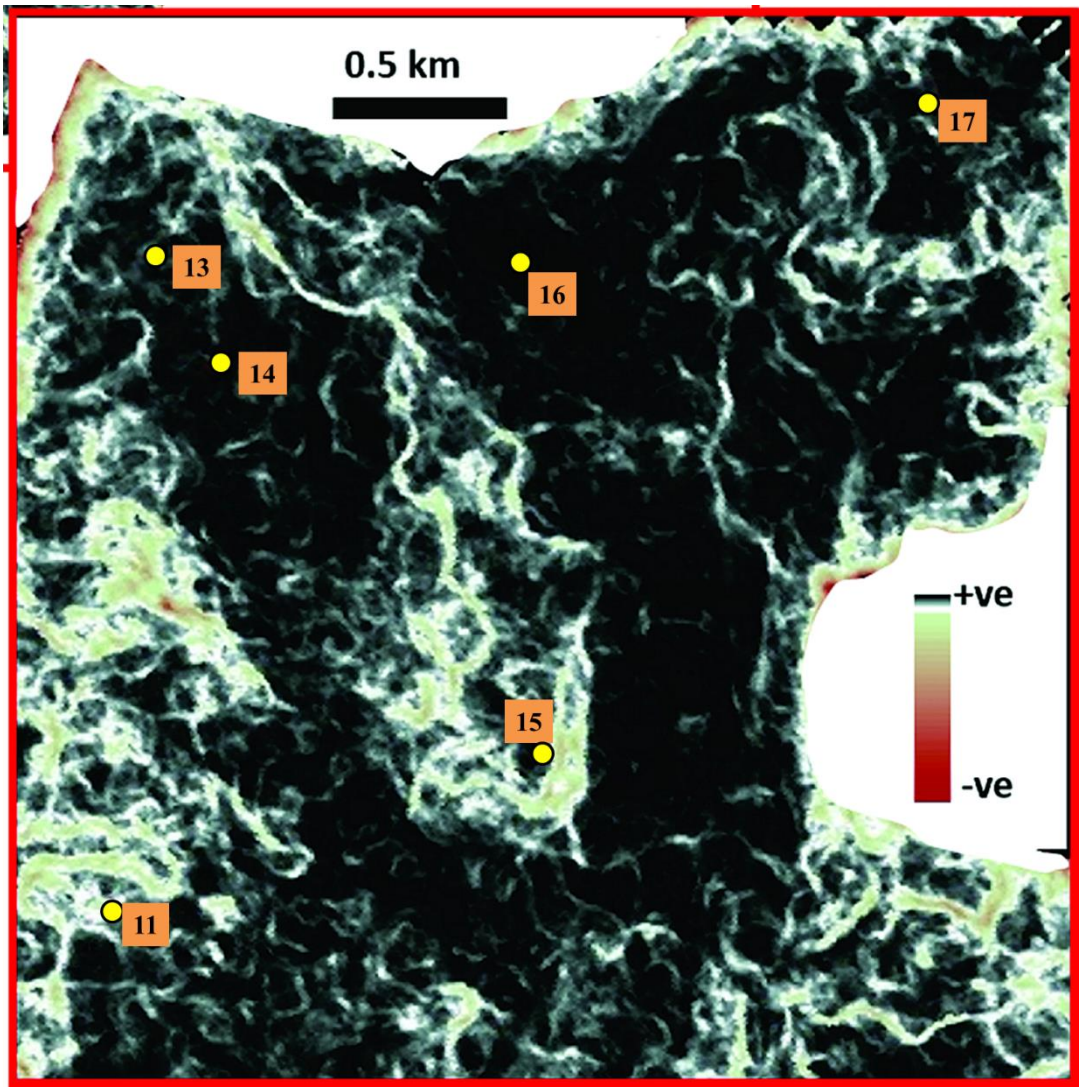

Figure 40b: Numerous channels present within the H7 interval

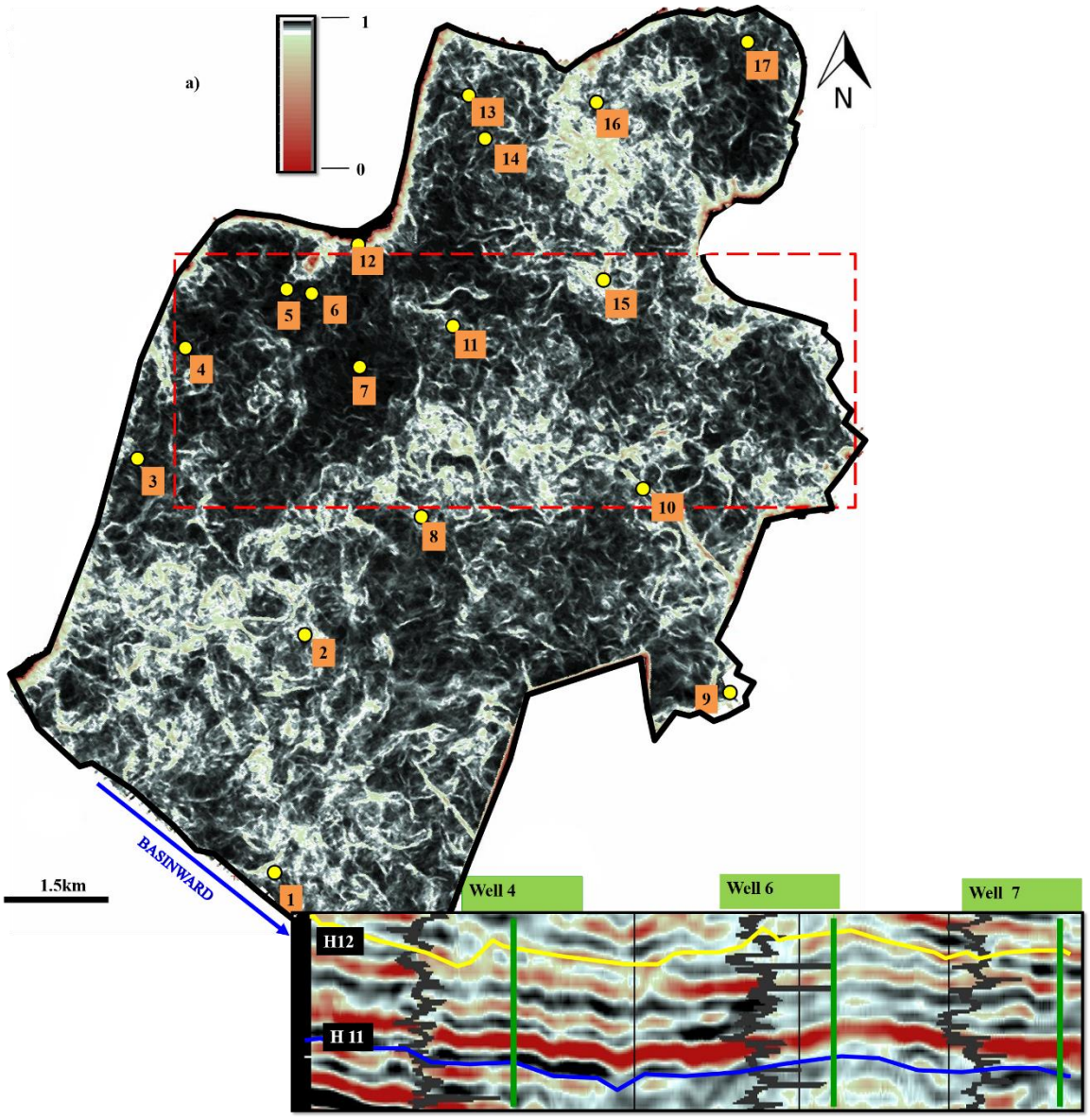

Figure 41a: Variance map for H11; larger valley scours appear in Younger intervals. Red dashed rectangle highlights some incisional features. See figure 41b.

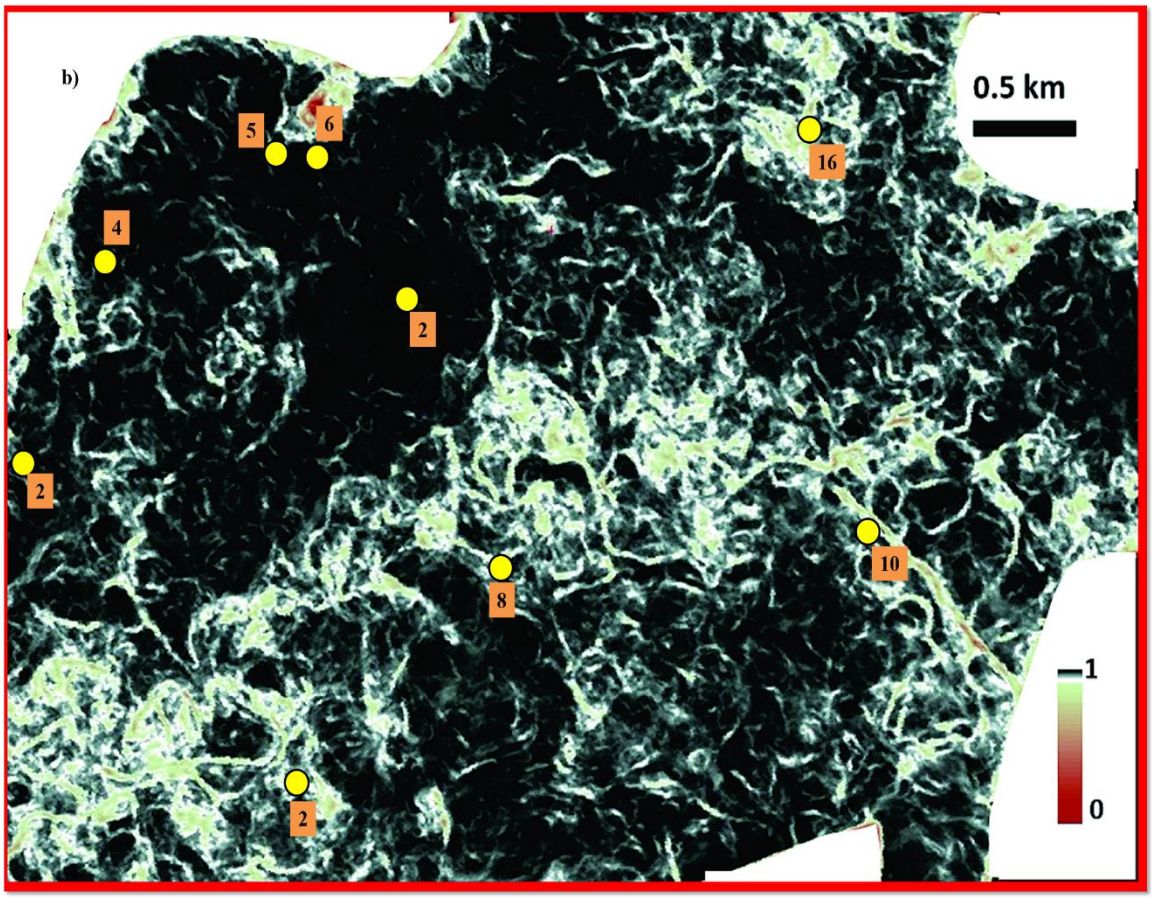

Figure 41b: Large west-east trending incisional features in H11 .

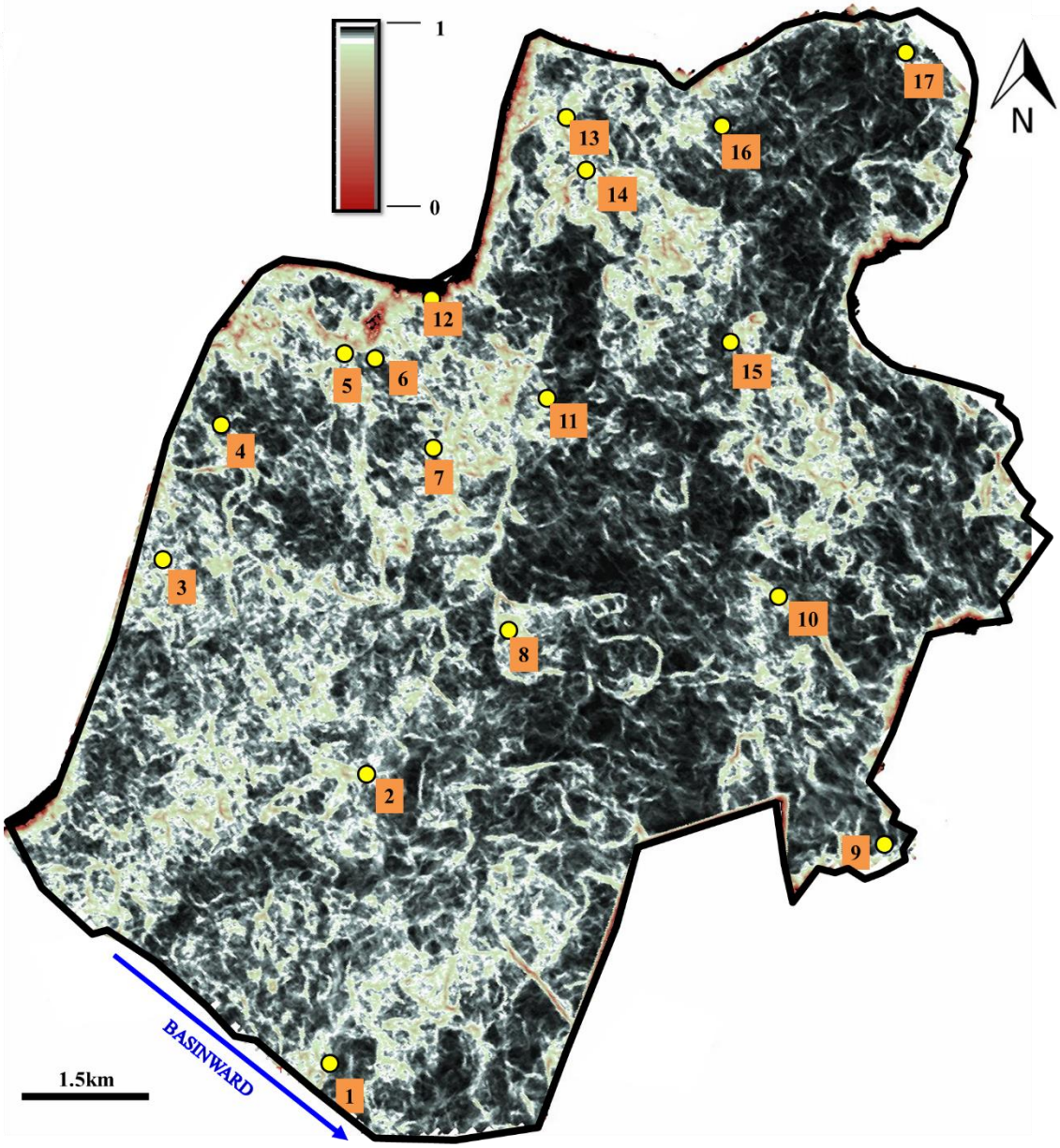

Figure 42: Variance map for H15 showing channels and valley cuts

DISCUSSION AND CONCLUSIONS

Analysis of the morphological pattern of seismically imaged stratigraphic features and associated deposits provides information about its depositional processes. The study interval includes the Oakville Sandstone that marks the basal Miocene and the overlying Fleming formation. The seismically imaged stratigraphic maps show that after the Anahuac Shale Formation, the coastline was built of prograding beach ridges characteristic of a wave dominated coast and considerable alongshore transport and accumulation of sand. The beach ridges have the greatest volume of sand within the section, and this is a common occurrence of any early Miocene coastal depositional system. Galloway et al. (2000), Galloway, (1987, 1999) reported that sediment provenance during the Lower Miocene was from the North Padre and Norma deltaic complexes on the northeast and the Calcasieu and Mississippi deltas on the southwestern axes of the GOM. (See figure 5).

The fluvially dominated coastal section was first dominated by channel belts and later by incised valleys and channel belts. Channels remained characteristically sinuous and single-thread through the section. Evidence of rapid transgressions and regression in map view are rare. The only example is shown in Figure 38; rapid transgressions and regressions do not produces regionally preserved stratigraphy because much of the strata appear to be cut out by later channel belts and valleys.

The change from strandplain to fluvial environment is characterized by changes in sedimentary structures, appearance of channels and incised valley cuts. Sinuous, single-thread fluvial channel deposits appear to dominate the stratigraphy of the non-marine environments characterizing the overall coastal progradation recorded by the Lower Miocene strata. The dip orientated channels extend to the edge of the study area

and do not show signs of thinning out (Figure 43). It is evident that, they served as sediment supply to the prograding coast and at the largest scale to the Cenozoic shelf-margin out-build. The subtle change in style of valley walls as we move up the section, suggest the change in channel character. In addition, increase in width of the valleys indicates further in-land position of the younger strata.

The alternating wireline signatures from upward coarsening to upward fining, reveals the repetitive Cenozoic depositional pattern described by previous studies in other parts of the Gulf basin (Galloway 1989, Loucks et al. 2011, Fongngern and Ambrose, 2012). Fluvial to delta to delta-fed apron and coastal plain to shore-zone to shelf to shelf-fed apron, are the depositional systems groups that were observed within the study as categorized by (Galloway et al. 2000) for the Cenozoic genetic sequences of the Gulf basin.

Interpretation of this data leaned more on the amplitude variance maps generated. Well logs were widely spaced and few and these hindered regional strata correlations. The map patterns largely show a regressive depositional history dominated by a shorezone system and younger channels, channel belts and incised valleys. The observed stratigraphy and structures also reveal that the San Marcos Arch was not active during the Lower Miocene.

The stratigraphic evidence includes

(1) Straight beach ridges that suggest the arch is not adding local curvature to the coastline.

(2) Channel belts that show no evidence of deflection in orientation by a potential topographic high.

(3) Incised valleys that display no spatial change in scale that might be expected by relative arch uplift to the northeast.

The structural evidence for no arch activity during the Lower Miocene is no large scale change in sediment thickness from southwest to northeast that would be expected by a subsidence pattern associated with active arch tectonism.

REFERENCES

Ambrose, A.W. and Tyler N., 1985, Facies architecture and production characteristics of strandplain reservoirs in the Frio Formation, Texas. Bureau of Economic Geology. Report of Investigations No. 146.

Bhattacharya, J.P. and Walker, R.G., 1991, Facies and facies sucessions in river and wave dominated depositional systems of the Upper Cretaceous Dunvegan Formation, northwestern Alberta. Bulletin of Canadian Petroleum Geology, v. 39, no.2 p. 165-191.

Bhattacharya, J.P., 1993, The expression and interpretation of marine flooding surfaces and erosional surfaces in core; examples from the Upper Cretaceous Dunvegan Formation, Alberta foreland basin, Canada. Special Publication International Association sedimentologist, v. 18,p. 125-160

Bhattacharya,,J.P.and Giosan, L., 2003,Wave–influenced deltas: geomorphological implications for facies reconstruction. Sedimentology v. 50, p. 187-210.

Bhattacharya, J. P, 2006, Deltas. Facies Models revisited, Society for Sedimentary Geology (SEPM) Special Publication No.4, p. 237-292.

Boyd, R., Dalrymple R., and Zaitlin, B.A., 1992, Classification of clastic coastal depositional environments. In: Donoghue J.F, Davis R.A, Fletcher C.H. and Suter J.R. (Editors), Quaternary Coastal Evolution. Sedimentary Geology, v. 80, p. 139-150.

Dalrymple, R.W., Zaitlin, B.A., and Boyd, R., 1992, Estuarine facies models: conceptual basis and stratigraphic implications. SEPM, Journal of sedimentary petrology, v. 62, no. 6, p. 1130-1146.

Owen, D.E., 2008, Geology of the Chenier Plain of Cameron Parish, southwestern Louisiana. ed.: Geological Society of America Field Guide 14, 2008 Joint Annual Meeting, Houston, Texas, p. 27–38

Clifton, H.E., 2006, A reexamination of facies models for clastic shorelines. In: Posamentier, HW, and Walker, RG, eds, Facies Models Revisited: SEPM, Special Publication, v. 84, p. 293–337.

Congxian, Li, Ping Wang, Daidu Fan and Shouye Yang, 2006, Characteristics and Formation of Late Quaternary incised-valley-fill sequences in sediment-rich deltas and estuaries: Case studies from C hina SEPM Special Publication No. 85, p. 30

Fisher, W.L., Brown, L.F., Scott, A.J. and McGowen, J.H., 1969. Delta Systems in the Exploration for Oil and Gas. Bur. Econ. Geol., University of Texas, Austin, p. 78.

Galloway, W. E., and Hobday, D. K., 1983, Terrigenous clastic depositional systems. Applications to petroleum, coal and uranium exploration: Springer-Verlag,New York, NY, pp. 7, 420.

Galloway, W. E., and Cheng, E.S., 1985, Reservoir facies architecture in a microtidal barrier system— Frio Formation, Texas Gulf Coast: The University of Texas at Austin, Bureau of Economic Geology Report of Investigations No. 144, p36 In: William E. Galloway 1987, Depositional and structural architecture of prograding clastic continental margins: tectonic influence on patterns of basin filling. Norsk Geologisk Tidsskrift, Vol. 67, pp. 237-251. Oslo 1987. ISSN 0029-196X.

Galloway, W. E., 1989, Genetic stratigraphic sequences in basin analysis II: Application to Northwest Gulf of Mexico Cenozoic basin. AAPG Bulletin, v. 73, no. 2p. 143-154.

Galloway, W. E., Ganey-Curry, P., Xiang Li, and Richard, T. B., 2000, Cenezoic depositional history of the Gulf of Mexico basin. AAPG Bulletin, v. 84, no. 11 p. 1743-1774.

Galloway, W. E., 2008, Depositional Evolution of the Gulf of Mexico Sedimentary Basin. Sedimentary Basins of the World, v. 5 p. 505- 549.

Galloway, W. E., Whiteaker, T. L. and Ganey-Curry, P., 2011, History of Cenozoic North American drainage basin evolution, sediment yield, and accumulation in the Gulf of Mexico basin. Geological Society of America Geosphere, v.7 no. 4 p. 938-973.

Gibling, R. M., 2006, Width and thickness of fluvial channel bodies and valley fills in the geological record: A literature compilation and classification. SEPM, v. 76, p.731-770.

Goodbred, S.L. and Saito, Y., 2012, Tide dominated deltas. In: R.A Davis Jr. and R.W. Dalrymple (eds), Principles of Tidal Sedimentology: Springer science and Business media.

Halbouty M. T., 1966, Stratigraphic-Trap Possibilities in Upper Jurassic Rocks, San Marcos Arch, Texas. American Association of Petroleum Geologist. v. 50 pp. 3-24.

Olariu C., 2014, Estuaries and Incised valleys. Clastic Depositional Systems. Personal Communication.

Posamentier, H.W. and Allen, G.P., 1993, Variability of the sequence stratigraphic model: effects of local basin factors: Sedimentary Geology, v. 86, p. 91–109. In Cornel Olariu, C., 2014, Clastic Depositional Systems. Personal communication.

Rattanaporn, F., 2011, Sequence Stratigraphy, Sandstone Architecture, and Depositional Systems of the Lower Miocene Succession in the Carancahua Bay Area, Texas Gulf Coast. Master's Thesis, The University of Texas at Austin. p.56

Rattanaporn, F. and Ambrose, W. A., 2012, Variability of Sandstone Architecture and Bypass Systems of the Miocene Oakville and Lower Lagarto Formations in the Carancahua Bay Area, Texas Gulf Coast. Gulf Coast Association of Geological Societies Transactions, v. 62, p. 131–144.

Robert, G. L., Brian, T. M., and Hongliu. Z., 2011, On-shelf lower Miocene Oakville sediment-dispersal patterns within a three-dimensional sequence-stratigraphic architectural framework and implications for deep-water reservoirs in the central coastal area of Texas. AAPG Bulletin, v. 95, no. 10, p. 1795–1817.

Subrahmanyam, D. and Rao, P.H., 2008, Seismic attributes –A review. 7th International Conference & Exposition on Petroleum Geophysics.

Vail, P. R., Hardenbold, J., and Todd, R. G., 1984. Jurassic unconformities, chronostratigraphy, and sea-level changes from seismic stratigraphy and biostratigraphy. In: Schlee J. S. (Ed), Interregional unconformities and Hydrocarbon Accumulation. American Association of petroleum Geology, Memoir v. 36 p. 129-144.

Van Wagoner, J.C., Posamentier, H. W., Mitchum, R. M., Vail, P.R., Sarg, J.F., Loutit, T.S. and Hardenbol, J., 1988, An overview of sequence stratigraphy and key definitions. In: C.W. Wilgus et al., eds., Sea level changes: an intergrated approach. Society of Economic Paleontologists and Mineralogists Special Publication v.42 p. 39-45.

Van Wagoner, J. C., Mitchum, R. M, Campion, K. M., and Rahmanian, V. D., 1990, Siliciclastic sequence stratigraphy in well logs, cores, and outcrops: AAPG Methods in Exploration series 7, p.55.

Walker, R. G. and Plint, A. G., 1992, Wave and Storm dominated shallow marine systems, in: Walker, R. G. and James, N. P. (eds), Facies Models, response to sea level change. Geological Association of Canada, p. 219-238.

Winker C.D., 1982, Cenozoic shelf margins, northwestern Gulf of Mexico basin: Gulf Coast Association of Geological Societies Transactions, v. 32, p. 427-448. In: William E. Galloway, 1989, Genetic stratigraphic sequences in basin analysis II:

Application to Northwest Gulf of Mexico Cenozoic basin. AAPG Bulletin, v. 73, no. 2p. 143-154.

Zaitlin, B.A., Dalrymple, R.W., and Boyd, R., 1994, The stratigraphic organization of incised-valley systems associated with relative sealevel change, in Dalrymple, R.W., Boyd, R., and Zaitlin, B.A., eds., Incised-Valley Systems: Origin and Sedimentary Sequences: SEPM, Special Publication 51, p. 45–62.

Gulf of Mexico Basin Cenozoic Chronostrostragraphic Designations and Biostratigraphic Datums Chart, 2013. Version 18, Gulf of Mexico Basin Depositional Synthesis (GDBS). The University of Texas at Austin